Classical Theory of the Ground Spin-State in Cubic Spinels

D. H. LYONS,* T. A. KAPLAN, K. DWIGHT, AND N. MENYUK
Lincoln Laboratory,† Massachusetts Institute of Technology, Lexington, Massachusetts
(Received November 13, 1961)

An investigation of the classical Heisenberg exchange energy has led to the discovery of a new spin configuration, called a ferrimagnetic spiral. The explicit construction of this state is accomplished by application of the Lyons-Kaplan generalization of the Luttinger-Tisza method (GLT). For all B-B interactions which are sufficiently large to destabilize the Néel (collinear) configuration, this spiral has lower energy than all previously proposed spin configurations including those of Néel and Yafet-Kittel. Furthermore, this ferrimagnetic spiral is found to be stable against arbitrary small deviations of the spin vectors over a range of interactions that is contiguous with the Néel range. It is also shown, by further application of the GLT method, to have the lowest energy over an additional large class of spin configurations. In view of these results, it is likely that the ferrimagnetic spiral is the ground state over its range of local stability.

The complete class of configurations possessing "equal relative angles" (i.e., invariance of the angles between spins under lattice translations) is elucidated for the first time. It is shown that the ferrimagnetic spiral has the lowest energy over this class of configurations for a range of interactions which includes the range of stability, and extends beyond it. It follows that for interactions in the latter range, the relative angles in the ground state must not possess translational invariance, in contradiction to earlier hypotheses.

The neutron diffraction pattern resulting from general magnetic spirals is discussed. The striking agreement between our theoretical results and the complex pattern found by Corliss and Hastings for manganese chromite supports the theory. In addition, the spin configuration at the Curie point, in the molecular field approximation, is shown to be in accord with the observed temperature dependence in manganese chromite.

I. INTRODUCTION

RECENT experiments[1,2] on spinel structures have revealed the presence of spin configurations which are neither of the Néel[3] nor of the Yafet-Kittel[4] types. Although these experimental results are not necessarily inconsistent[5] with the classical Heisenberg theory of spin-configurational energy, it is important to determine whether or not they are consistent. In this paper, we shall first describe an attempt to rigorously find the ground state of the classical Heisenberg energy,[6] assuming reasonable exchange interactions. We then discuss some of the ramifications of our results.

We shall restrict ourselves to the consideration of spinels where all the B-site cations are of one ionic specie and all the A-site cations of another (i.e., normal spinels), where the crystal symmetry is cubic (as discussed in Appendix I),[7] and where only nearest-neighbor A-B and B-B antiferromagnetic interactions (J_{AB} and J_{BB}, respectively) are present.[8] Then the ground state depends only upon the parameter u defined by[9]

$$u=(4J_{BB}S_B)/(3J_{AB}S_A). \quad (1)$$

The Néel configuration (A-site spins parallel to each other and antiparallel to the B-site spins) is the ground state for sufficiently small values of this parameter u, namely, for $u\leqslant u_0=8/9$.[10,11] This result was proved rigorously in reference 11 by using the generalized Luttinger-Tisza (GLT) method described therein, and our present effort to discover the true ground state for $u>u_0$ involves further application of the GLT method. A survey of many of the results of this investigation has already been given,[9] but without the necessary details and proofs, which are included in the treatment below.

The initial steps in our procedure lead to a low-energy state of the magnetic-spiral type.[12] The energy of our spiral lies appreciably lower than that of the Yafet-Kittel state. Furthermore, it satisfies the rather stringent, necessary condition that the energy of any proposed ground state for a range of u contiguous to u_0 must lie lower than that of the Néel state whenever the latter is unstable. The subsequent steps in the application of the GLT method are directed toward proving the above spiral to be the ground state, and in this respect

---

* Now at Sperry-Rand Research Center, Sudbury, Massachusetts.

† Operated with support from the U. S. Army, Navy, and Air Force.

[1] J. Hastings and L. Corliss, Phys. Rev. **126**, 556 (1962).

[2] E. Prince, J. Appl. Phys. **32**, 68S (1961).

[3] L. Néel, Ann. Phys. **3**, 167 (1948).

[4] Y. Yafet and C. Kittel, Phys. Rev. **87**, 290 (1952).

[5] Since overly restrictive sublattice restrictions were made by Néel and by Yafet-Kittel. See T. A. Kaplan, Phys. Rev. **116**, 888 (1959).

[6] It should be realized that the result of this classical ground state problem is of fundamental importance in the standard approximate quantum-mechanical theories: the molecular (or internal) field and the spin-wave approximations. In the molecular field approximation to the ground state, the wave function for the nth spin is quantized along a direction $\hat{z}_n$, which is given by the solution to the classical problem. The value of $\hat{z}_n\cdot\mathbf{S}_n$ in this state is S_n, the spin quantum number for the nth ion. In the spin-wave approximation, it is $\hat{z}_n\cdot\mathbf{S}_n$, the component of the nth spin operator along the classical direction, which is taken to be large (of the order S_n).

[7] We define crystal symmetry as the symmetry of the crystal without spin directions.

[8] These restrictions appear reasonable, since materials exist which *a priori* might be expected to satisfy them. However, they are not essential, since our approach requires only that every ionic specie be ordered in the crystal.

[9] T. A. Kaplan, K. Dwight, D. H. Lyons, and N. Menyuk, J. Appl. Phys. **32**, 13S (1961).

[10] T. A. Kaplan, Phys. Rev. **119**, 1460 (1960).

[11] D. H. Lyons and T. A. Kaplan, Phys. Rev. **120**, 1580 (1960).

[12] The magnetic spiral referred to here can be ferrimagnetic [see Eq. (9)]. They were first introduced in connection with distorted spinels at the Gatlinberg Conference on Neutron Diffraction by T. A. Kaplan, K. Dwight, and N. Menyuk, Bull. Am. Phys. Soc. **5**, 460 (1960). Such a spiral was subsequently found in erbium by W. C. Wilkinson, W. C. Koehler, E. O. Wollan, and S. W. Cable, J. Appl. Phys. **32**, 48S (1961).

our effort fails. However, this application succeeds in proving that our magnetic spiral is the best over a large and precisely defined class of spin configurations. In addition, it yields a rigorous lower bound to the ground-state energy.

Another stringent necessary condition for a configuration to be the ground state is that of local stability, i.e., stability with respect to arbitrary small deviations of all the spin vectors from their direction in the configuration of interest. It is shown that our spiral is locally stable for $u_0<u<u''\cong 1.3$, and unstable for $u>u''$. In addition, that mode of spin deviations which most rapidly destabilizes the magnetic spiral for u slightly larger than u'' has been determined, and the ensuing configuration is shown to be ordered in a complicated manner.

To put these results succinctly, we have found a spin configuration which might be (and, subjectively speaking, is likely to be) the ground state for $u_0\leqslant u<u''$, and which is definitely not the ground state for $u>u''$. In at least part of the latter region, the true ground state must be more complicated than our magnetic spiral, as suggested by the small-deviation mode mentioned above, and as shown by the detailed consideration of the GLT method.

In the literature, various invariance hypotheses[13,14] have sometimes been used to restrict the class of possible ground-state spin configurations. In Appendix V, we elucidate all those configurations which possess "equal relative angles," i.e., where $\mathbf{S}(\mathbf{R})\cdot\mathbf{S}(\mathbf{R}')$ is invariant under the lattice translations. Then further consideration of the GLT method yields a proof that the magnetic spiral previously constructed has the lowest energy of all such equal-relative-angle configurations even for some $u>u''$, so that there exist values of u for which the ground-state spin configuration cannot possess equal relative angles. It is pointed out that this result should not be surprising, despite existing inductive evidence, since there is no *a priori* reason to expect any such invariance hypothesis to be true in general.

The most direct experimental means of ascertaining the actual ground-state spin configuration is by neutron diffraction. The calculation of the diffraction patterns resulting from the configurations considered in this paper follows most conveniently from a general expression involving the Fourier transforms of the spins. This general expression leads to many additional scattering points in reciprocal space even for as simple a spin configuration as a ferrimagnetic spiral. These extra scattering points considerably increase the difficulty of deducing an appropriate spin configuration from experimental data, as is illustrated by the explicit details for our magnetic spiral. Thus, some theoretical insight into the type of configuration to be expected becomes virtually essential for an interpretation of the experimental results.

Finally, our theoretical findings are compared with the experimental results for manganese chromite.[1] If the spiral model is used to interpret the measured magnetization, the appropriate value for u ($\cong 1.6$) is greater than u''. Nevertheless, there are striking qualitative similarities between the observed diffraction pattern and that predicted for our magnetic spiral. This agreement supports our assumption of the classical Heisenberg energy, as well as our belief that the spiral is the ground state for $u_0\leqslant u<u''$. It also suggests that the spiral approximates the ground state for u as large as 1.6. The fact that a spiral can only be an approximation in manganese chromite is one of the plausible explanations given for the discrepancies between the observed pattern and that predicted for our spiral. In addition, the high-temperature spin configuration is calculated in the molecular field approximation, and it implies a Néel-magnetic spiral transition which appears to be consistent with the available data.

II. APPLICATION OF THE GLT METHOD

A. Construction of the [110] Solution

The classical Heisenberg energy can be expressed[9] as

$$E=\sum_{n\nu,m\mu}\bar{J}_{n\nu,m\mu}\mathbf{S}_{n\nu}\cdot\mathbf{S}_{m\mu}, \tag{2}$$

where n, m identify the unit cell; ν, μ identify the particular site within a unit cell; $S_{n\nu}$ is a unit vector in the direction of the spin on the $n\nu$th site; and $\bar{J}_{n\nu,m\mu}=S_\nu S_\mu J_{n\nu,m\mu}$, S_ν being the spin magnitude for the $n\nu$th site and $J_{n\nu,m\mu}$ being the negative of the usual exchange integral. Our problem consists of finding a set of unit vectors $\mathbf{S}_{n\nu}$ which minimizes this energy for normal cubic spinels. The search for such a solution might appear hopeless, since there is an enormous number of individual spins in a crystal and since there is no *a priori* restriction on the direction of any of these spins, as noted in Appendix I. Nevertheless, the GLT method is able to solve this problem rigorously[11] for $u\leqslant u_0$.

A thorough discussion of the GLT method has already been given.[11] We recall here that the technique involves finding the minimum (over $\mathbf{k}$ and over the six branches $\alpha=1, 2, \cdots 6$) of the eigenvalues $\lambda_\alpha(\mathbf{k})$ of the matrices defined by

$$\mathfrak{L}_{\nu\mu}(\mathbf{k})=\beta_\nu\beta_\mu L_{\nu\mu}(\mathbf{k}), \tag{3}$$

where

$$L_{\nu\mu}(\mathbf{k})=\sum_m \bar{J}_{n\nu,m\mu}\exp[i\mathbf{k}\cdot(\mathbf{R}_{m\mu}-\mathbf{R}_{n\nu})], \tag{4}$$

the $\mathbf{R}_{n\nu}$ being vectors from the origin to the $n\nu$th site. $\mathbf{L}(\mathbf{k})$ is given explicitly in Appendix II, both for general $\mathbf{k}$ and for $\mathbf{k}=k[110]/\sqrt{2}$. The β_ν are arbitrary real parameters which are to be chosen so that the spin configuration constructed from eigenvectors associated with the minimum eigenvalues of $\mathfrak{L}(\mathbf{k})$ consists of unit spin vectors (i.e., satisfies the so-called "strong con-

[13] H. A. Gersch and W. C. Koehler, J. Phys. Chem. Solids **5**, 180 (1958).

[14] E. F. Bertaut, Compt. rend. **250**, 85 (1961).

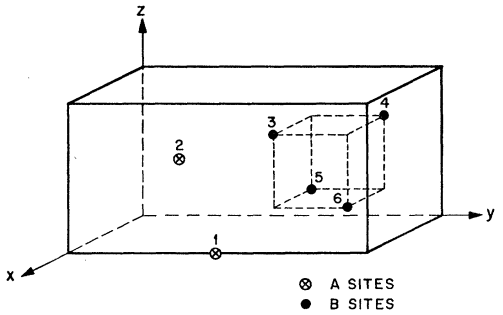

FIG. 1. The sites in a primitive unit cell of the spinel structure. The numbers $\nu=1, 2, \cdots, 6$ identify the various sites.

straints" $|\mathbf{S}_{n\nu}|=1$). If such β_ν can be found, then the method rigorously proves that the resulting configuration is the true ground state, and is said to work.

For $u \lesssim u_0$, the β_ν can be chosen[11] so that the minimum eigenvalue over all $\mathbf{k}$ and α is

$$\lambda_0=\min_\alpha \lambda_\alpha(0), \tag{5}$$

and the corresponding eigenvector satisfies the strong constraints. Thus the GLT method works, and the corresponding configuration (Néel) is thereby proven to be the ground state. This proof breaks down for $u>u_0$ because another eigenvalue, $\lambda_1(k_0[110]/\sqrt{2})$, becomes degenerate with λ_0 at $u=u_0$ [10,11] and lies lower than λ_0 for larger values of u. The corresponding configuration fails to satisfy the strong constraints. In other words, the method fails for this choice of the β_ν when $u>u_0$.

Such behavior suggests that the device of "forced degeneracy"[11] be used to satisfy the constraints, i.e., that the β_ν be chosen so as to retain the degeneracy of λ_0 with

$$\lambda_1(\mathbf{k}_0)=\min_{\alpha,k>0}\lambda_\alpha(k[110]/\sqrt{2}) \tag{6}$$

for $u \gtrsim u_0$. At this point in the calculation we temporarily ignore all eigenvalues corresponding to $\mathbf{k}$ in directions other than the [110], and hence restrict ourselves to the [110] class of configurations, i.e., to those configurations which can be constructed from arbitrary linear combinations of any number of Fourier components associated exclusively with $\mathbf{k}$'s in the [110] direction. Accordingly, it is convenient to restrict the choice of the β_ν so that $\mathfrak{L}(k[110]/\sqrt{2})$ retains the symmetry of $\mathbf{L}(k[110]/\sqrt{2})$, i.e., so that the matrices $\mathfrak{L}(k[110]/\sqrt{2})$ are also partially diagonalized into 1×1, 2×2, and 3×3 submatrices by transformation into the ψ_μ basis described in Appendix II. This requirement yields

$$\begin{aligned}&\beta_1=\beta_2=1,\\ &\beta_3=\beta_4=\beta'(u),\\ &\beta_5=\beta_6=\beta(u),\end{aligned} \tag{7}$$

where the sublattice labeling is shown in Fig. 1.

It should be noted that restricting our choice of β_ν places no restriction on the physically possible configurations under consideration (i.e., configurations satisfying the strong constraints). It only restricts the set of configurations which do not satisfy the strong constraints, since minimization of the energy over a weak constraint includes consideration of all physical states, regardless of the choice of the weak constraint. Thus, any information concerning physical states which is obtained from consideration of a particular weak constraint is rigorous, and cannot be contradicted by another choice of β_ν.

$\lambda_1(\mathbf{k}_0)$ arises from the 3×3 submatrices, and its definition as the minimum over $\mathbf{k}$ supplies one relationship among the three unknowns β, β', and $\mathbf{k}_0$. The forcing of the equality $\lambda_0=\lambda_1(\mathbf{k}_0)$ yields a second equation involving these variables. As a result of this forced degeneracy, the spin configuration can be constructed[11] from a linear combination of the corresponding eigenvectors, ψ_0 and $\psi_1(\mathbf{k}_0)$, which have the general form given by Eq. (B7). If one assigns ψ_0 to $S_{n\nu}{}^{z'}$ and $\psi_1(\mathbf{k}_0)$ to $S_{n\nu}{}^{x'}$ and $S_{n\nu}{}^{y'}$, then the strong constraints can be written explicitly in terms of the components of these eigenvectors. This procedure gives rise to three more equations involving β, β', $\mathbf{k}_0$, and two new variables which are the constants defining the linear combination. After a considerable amount of algebra, the simultaneous solution of the five equations described above can be reduced to the computational procedure given in Appendix III.

For $u>2$, the equations in Appendix III become inconsistent with the requirement that the β_ν be real,[11] and hence the foregoing calculation is valid only for $u_0 \lesssim u \lesssim 2$. However, examination of the six branches $\lambda_\alpha(k[110]/\sqrt{2})$ shows that the entire (flat) branch λ_2 (arising from the 1×1 submatrix) becomes degenerate with λ_0 and $\lambda_1(\mathbf{k}_0)$ at $u=u_1=2$. Following this suggestion, the functions $\beta(u)$ and $\beta'(u)$ are now chosen so as to retain the threefold degeneracy

$$\lambda_0=\lambda_1(\mathbf{k}_0)=\lambda_2 \tag{8}$$

for $u \gtrsim 2$. Simultaneous solution of the three relationships given by Eqs. (6) and (8) yields explicit expressions for $\beta(u)$, $\beta'(u)$, and $\mathbf{k}_0$. Then the three coefficients defining the linear combination of the corresponding eigenvectors suffice to satisfy the strong constraints, for $u_1 \lesssim u \lesssim u_2=3.817\cdots$.

At $u=u_2$, the coefficient of the $\mathbf{k}=0$ component in the linear combination vanishes, and the strong constraints can no longer be satisfied in the above fashion for $u>u_2$. This situation suggests that the requirement on λ_0 be relaxed by retaining only the right-hand equality of Eq. (8). The resulting equation, together with the definition of $\lambda_1(\mathbf{k}_0)$ and the strong constraints, again permits the determination of β, β', $\mathbf{k}_0$, and the coefficients of the linear combination of eigenvectors.

All of the configurations obtained above are of the magnetic spiral type[9] defined by

$$\begin{aligned}\mathbf{S}_{n\nu}=\sin\phi_\nu[&\hat{x}'\cos(\mathbf{k}_0\cdot\mathbf{R}_{n\nu}+\gamma_\nu)\\ &+\hat{y}'\sin(\mathbf{k}_0\cdot\mathbf{R}_{n\nu}+\gamma_\nu)]+\hat{z}'\cos\phi_\nu,\end{aligned} \tag{9}$$

where the orientation of the $\hat{x}'$, $\hat{y}'$, $\hat{z}'$ coordinate system with respect to the crystal axes is arbitrary. Note that the spins on each sublattice lie on a cone of half-angle ϕ_ν, with their positions on this cone determined by the other spiral parameters $\mathbf{k}_0$ and γ_ν. The calculated values of these parameters for $u \geqslant u_0$ are given in Fig. 2, where

$$\begin{aligned} &\phi_1=\phi_2, \quad \gamma_1=\gamma_2=0, \\ &\phi_3=\phi_4, \quad \gamma_3=-\gamma_4, \\ &\phi_5=\phi_6, \quad \gamma_5=\gamma_6=\pi. \end{aligned} \tag{10}$$

The equations by which these parameters are calculated are included in Appendix III for $u_0 \leqslant u \leqslant 2$, but are omitted for larger u because the configuration is locally unstable for $u>u''=1.298\cdots$, as found in Sec. III. Nevertheless, it should be emphasized that, for every value of u, a set of β_ν has been found such that configurations constructed from eigenvectors associated with the minimum (over α and k) eigenvalues of $\mathfrak{L}(k[110]/\sqrt{2})$ satisfy the strong constraints. Hence the GLT method "works" over the [110] class. This means that no spin configuration whatsoever composed entirely of Fourier components with $\mathbf{k}$'s in the [110] direction can yield a lower energy than the magnetic spiral determined above.

The energies of the Néel, Yafet-Kittel, and magnetic spiral configurations are compared in Fig. 3, which shows the spiral energy to lie significantly lower than the Yafet-Kittel result. It is interesting to note that both the energy and its first derivative with respect to u are continuous for all u, despite the changes in technique required at u_0, u_1, and u_2 and the associated discontinuities in the derivatives of the spiral parameters.

B. Investigation Over all k

In the course of constructing the minimum-energy spin configuration with Fourier components indexed by $\mathbf{k}$'s in the [110] direction exclusively, we have determined the corresponding values of the originally free parameters β_ν. These values define a particular set of $\mathfrak{L}(\mathbf{k})$ matrices. According to the GLT method, if our [110] spiral yields the minimum eigenvalue of this set of matrices, i.e., if

$$\lambda_1(\mathbf{k}_0) \leqslant \lambda_\alpha(\mathbf{k}) \text{ for all } \alpha \text{ and } \mathbf{k}, \tag{11}$$

then our spiral gives the absolute minimum energy for the original physical problem. However, a search over the Brillouin zone reveals some wave vectors $\mathbf{k}$ for which the above inequality is not satisfied, for all $u>u_0$.

Such a result does not in general imply that the configuration previously constructed is not the ground state.[15] Rather, it demonstrates the existence of lower-energy spin configurations which satisfy the "weak constraint"

$$\sum_{n,\nu} \beta_\nu^{-2} |\mathbf{S}_{n\nu}|^2 = N \sum_\nu \beta_\nu^{-2}, \tag{12}$$

but which do not necessarily satisfy the strong constraints $|\mathbf{S}_{n\nu}|=1$. Since all physically possible configurations (those which satisfy the strong constraints) are included amongst those satisfying the weak con-

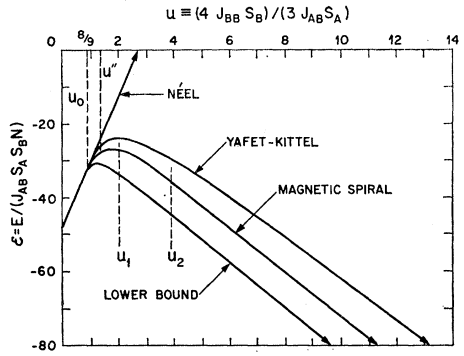

FIG. 3. Energy as a function of the parameter u for various spin configurations in normal cubic spinels.

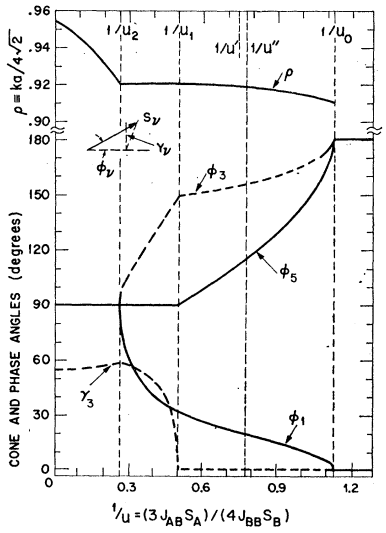

FIG. 2. Magnetic spiral parameters for normal cubic spinels. Together with the relationships given in Eq. (10), these values completely define the spin configuration as a function of u, according to Eq. (9).

[15] For $u>u_2$, the spiral is coplanar, in which case failure of the GLT method does imply that the configuration is unstable and cannot be the ground state. To prove this, we note that one of the coordinate vectors in Eq. (17) say $\boldsymbol{\eta}_{n\nu}$, can be chosen perpendicular to the plane of the spins, so that $\boldsymbol{\eta}_{n\nu}=\boldsymbol{\eta}$ and is independent of n and ν. Then from Eq. (D2) it follows that $F_{n\nu,m\mu}{}^{\eta\eta}=(\bar{J}_{n\nu,m\mu}-\delta_{n\nu,m\mu}\lambda_{m\mu})$ and $F_{n\nu,m\mu}{}^{\eta\xi}=0$, so that $\mathbf{F}$ is partially diagonalized into $\eta\eta$ and $\xi\xi$ submatrices. From the equations of reference 11, it can be shown that the GLT matrix (before Fourier transformation) is given by $\mathfrak{J}_{n\nu,m\mu}=\beta_{n\nu}\beta_{m\mu}\bar{J}_{n\nu,m\mu}$ and that $\lambda_{m\mu}=\lambda\beta_{m\mu}^{-2}$, where λ is that eigenvalue of $\mathfrak{J}$ which corresponds to the initial equilibrium configuration in question. Finally, the energy change can be written in terms of a small-deviation matrix $\mathfrak{F}$ defined by $\mathfrak{F}_{n\nu,m\mu}{}^{\xi\xi'}=\beta_{n\nu}\beta_{m\mu}F_{n\nu,m\mu}{}^{\xi\xi'}$, which contains the submatrix $\mathfrak{F}^{\eta\eta}=\mathfrak{J}-\lambda\mathbf{I}$, $\mathbf{I}$ being the unit matrix.

If the configuration is locally stable, then by definition the submatrix $\mathfrak{F}^{\eta\eta}$ cannot possess negative eigenvalues, so that λ must be the minimum eigenvalue of $\mathfrak{J}$. Conversely, if λ is not the absolute minimum eigenvalue of $\mathfrak{J}$, then the submatrix $\mathfrak{F}^{\eta\eta}$ must possess a negative eigenvalue, so that the configuration is unstable. Thus we have proven that, whenever a coplanar configuration is locally stable, the GLT method works and proves it to be the ground state (reference 11); and that, whenever the GLT method fails for a coplanar configuration, it is unstable and cannot be the ground state. The above argument also proves that the destabilizing mode consists of deviations out of the plane of the spins.

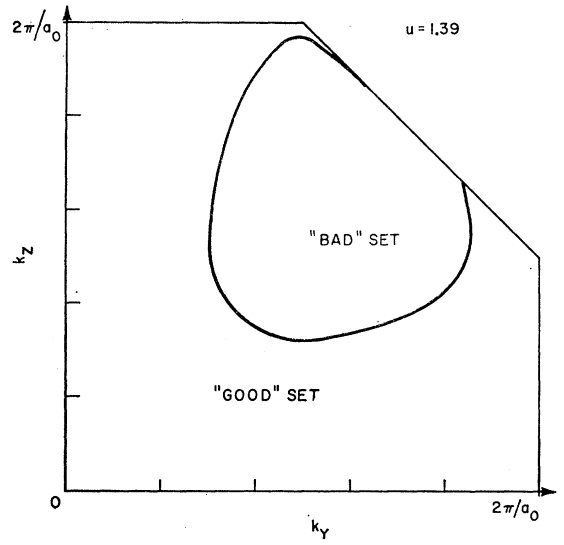

FIG. 4. Intersection of the plane $k_x=0$ with the "good" and "bad" sets for $u=1.39$.

straint, it follows that the minimum energy over the weak constraint always provides a lower bound to the energy of the true ground state. Thus the lower bound shown in Fig. 3 represents the minimum energy consistent with Eq. (12), but the corresponding configuration does not satisfy the strong constraints.

Furthermore, despite its failure to prove that the [110] spiral is the ground state, the GLT method is able to prove some other significant properties of this configuration. Let us define the "good" set as consisting of all $\mathbf{k}$'s in the first Brillouin zone[16] for which Eq. (11) is satisfied, and the "bad" set as consisting of all $\mathbf{k}$'s for which it is not. For the normal cubic spinel, this bad set consists of one region surrounding $\mathbf{k}=k_0[\bar{1}10]/\sqrt{2}$ together with another region surrounding $\mathbf{k}=k_0[011]/\sqrt{2}$. These two regions are small when $u-u_0$ is small, but grow as u increases. Nevertheless, the good set still fills most of the Brillouin zone at $u=1.39$, as illustrated in Fig. 4 for the $k_x=0$ plane. It follows from the theory of the GLT method that *the* [110] *magnetic spiral constructed above yields the absolute minimum energy over all configurations composed of Fourier components drawn exclusively from the "good" set.* It should be noted that this "good" set includes the [110] class considered above, but it goes far beyond this limited class.

As can be seen from Eq. (9), the Fourier components of magnetic spirals are nonzero only for $\mathbf{k}=0$ and a single $\pm\mathbf{k}\neq 0$. In addition, it is clear that similar spirals constructed from any of the "cubic equivalents" of a given $\mathbf{k}$ all possess equal energies. Since a detailed examination shows that the "good" set contains at least one of the "cubic equivalents" of every k vector for all $u<u'\cong 1.35$, and since the [110] spiral gives the minimum energy over the "good" set, it follows that *the* [110] *spiral is the minimum-energy magnetic spiral for u at least as great as $u'\cong 1.35$.* This conclusion is not a trivial result, since the general magnetic spiral involves fourteen arbitrary parameters: three components of $\mathbf{k}$, six cone angles, and five phase angles (one phase being arbitrary).[17]

The GLT method also proves that, when $u=u_0$, the minimum energy is attained only by the Néel state, since the eigenvalue $\lambda_1(\mathbf{k}_0)$ and those degenerate with it by virtue of cubic symmetry are found to be the only ones degenerate with λ_0. Hence, every ground state for the weak constraint problem is a linear combination of these degenerate eigenstates. Furthermore it can be shown that the only such combination that satisfies the strong constraints yields the Néel configuration, so that when $u=u_0$, there is no other physical state that is degenerate with the Néel state. It follows that, in the exact ground state, each spin must move continuously from its position in the Néel state as u increases past u_0. Our [110] spiral satisfies this condition.

III. STABILITY OF THE [110] MAGNETIC SPIRAL

Application of the GLT method has enabled us to construct a [110] magnetic spiral which is the best [110] configuration, to prove that it yields the minimum energy over a larger class of spin configurations, to prove that it is the best magnetic spiral for $u<u'$, and to prove that it is not the ground state for $u\geqslant u_2$.[15] However, the above results neither prove that this [110] spiral is the true ground state for $u_0\leqslant u\leqslant u_2$, nor imply that it is not. Hence, we turn to an investigation of the local stability of the configuration to obtain further information.

A configuration is called locally stable if all arbitrary, but small, spin deviations increase the energy, except for those which correspond to uniform rotations of all the spins. To calculate this energy difference, let $\mathfrak{X}_{n\nu}$ represent a set of length-preserving spin deviations. Then

$$\mathbf{S}_{n\nu}'=\mathbf{S}_{n\nu}+\mathfrak{X}_{n\nu}, \tag{13}$$

with

$$(2\mathbf{S}_{n\nu}+\mathfrak{X}_{n\nu})\cdot\mathfrak{X}_{n\nu}=0, \tag{14}$$

where $\mathbf{S}_{n\nu}$ denotes an initial spin configuration, and $\mathbf{S}_{n\nu}'$ denotes that resulting from the deviations. If the initial configuration is an equilibrium state, it must satisfy

$$\sum_{m\mu}\bar{J}_{n\nu,m\mu}\mathbf{S}_{m\mu}=\lambda_{n\nu}\mathbf{S}_{n\nu}, \tag{15}$$

where $|\lambda_{n\nu}|$ is essentially the magnitude of the molecular field at the $n\nu$th site. Then from Eqs. (2), (13), (14), and (15), it follows that the difference in energy between the new (primed) configuration and the initial (unprimed) equilibrium configuration is

$$\Delta E=\sum_{n\nu,m\mu}(\bar{J}_{n\nu,m\mu}-\delta_{n\nu,m\mu}\lambda_{m\mu})\mathfrak{X}_{n\nu}\cdot\mathfrak{X}_{m\mu}. \tag{16}$$

[16] Because of the symmetry of $\mathfrak{L}(\mathbf{k})$, it is sufficient to consider only the eighth of the zone with $k_z>0$ and $-k_y<k_x<k_y$.

[17] Even with the assistance of a high-speed computer, the straightforward minimization of the energy with respect to these fourteen parameters would be a lengthy, if not impossible, task.

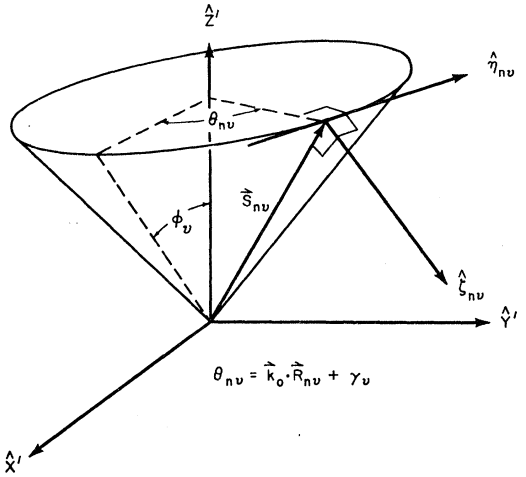

FIG. 5. Coordinate system used in the investigation of local stability. This system "moves" with the spins in the sense that each spin has its own individual coordinate system.

This expression is completely general, and involves no assumption as to the magnitudes of the spin deviations.

Let the initial equilibrium configuration be the [110] magnetic spiral determined in Sec. II(A). Then it can be shown[18] that $\lambda_{n\nu}=\beta_\nu^{-2}\lambda_1(\mathbf{k}_0)$. Noting that, from Eq. (14), $\varkappa_{n\nu}$ must be perpendicular to the initial spin $\mathbf{S}_{n\nu}$ to first order, we choose $\boldsymbol{\zeta}_{n\nu}$ and $\boldsymbol{\eta}_{n\nu}$ to be unit vectors orthogonal to each other and to the spin $\mathbf{S}_{n\nu}$, where $\boldsymbol{\eta}_{n\nu}$ is also perpendicular to the cone axis, as shown in Fig. 5. It follows that, to first order,

$$\varkappa_{n\nu}=\chi_{n\nu}{}^{\xi}\boldsymbol{\zeta}_{n\nu}+\chi_{n\nu}{}^{\eta}\boldsymbol{\eta}_{n\nu}. \tag{17}$$

A Fourier expansion of the components $\chi_{n\nu}{}^{\xi}$ ($\xi=\zeta,\eta$) leads, as shown in Appendix IV, to the following expression for the quadratic (lowest-order) terms of the change in energy:

$$\Delta E=\sum_{\mathbf{k}}\sum_{\xi,\xi'}\sum_{\mu,\nu}M_{\nu\mu}{}^{\xi\xi'}(\mathbf{k})A_\nu{}^{\xi}(\mathbf{k})A_\mu{}^{\xi'}(\mathbf{k}), \tag{18}$$

where the $\mathbf{M}(\mathbf{k})$ are 12×12 matrices given explicitly in Appendix IV. These matrices yield eigenvectors $\boldsymbol{\Phi}_\alpha(\mathbf{k})$ corresponding to eigenvalues $\mu_\alpha(\mathbf{k})$, with a minimum eigenvalue defined by

$$\mu_1(\mathbf{k}_1)=\min_{\alpha,\mathbf{k}}\mu_\alpha(\mathbf{k}). \tag{19}$$

In terms of the matrices $\mathbf{M}(\mathbf{k})$ defined by Eq. (18), the condition for local stability states that all of the eigenvalues of these matrices must be positive, except for those associated with uniform-rotational modes, which will be zero. An equivalent statement of this condition is that $\mu_1(\mathbf{k}_1)=0$, where $\mathbf{k}_1$ yields a uniform rotation: e.g., $\mathbf{k}_1=0$ or $\pm\mathbf{k}_0$ for a ferrimagnetic spiral. Numerical calculations performed with an IBM 709 computer showed this condition to be satisfied for all $u<u''=1.298\cdots$, and violated for all $u>u''$. Hence, *the* [110] *magnetic spiral is stable against small, but otherwise arbitrary, deviations of the spins for* $u<u''$. The fact that our [110] spiral satisfies this stringent requirement suggests that it is the ground state for $u<u''$, but it does not constitute a proof because metastable states of the Heisenberg energy do exist.[19]

For $u>u''$, some of the matrices $\mathbf{M}(\mathbf{k})$ develop negative eigenvalues, and hence the [110] spiral is unstable (and cannot be the ground state) over this region of u. At $u=u''$, $\mu_1(\mathbf{k}_1)=0$ and

$$\mathbf{k}_1a_0=2\pi(-0.0339,\,1.2016,\,0), \tag{20}$$

which does not correspond to a uniform rotation. The associated, unnormalized eigenvector is given by

$$\boldsymbol{\Phi}_1(\mathbf{k}_1)=(1,\,1,\,3.41,\,3.41,\,-0.35,\,-0.35,\,+1.15i,\,+1.15i,\,-2.86i,\,-2.86i,\,-2.04i,\,-2.04i), \tag{21}$$

where the components of $\boldsymbol{\Phi}_1(\mathbf{k}_1)$ correspond to the Fourier transforms of the small spin deviations according to Eq. (D7). (The convenience of placing $\mathbf{k}_0-\mathbf{k}_1$ within the first Brillouin zone forces $\mathbf{k}_1$, as given by Eq. (20), outside the zone. There is, of course, an equivalent interior value determined from $\mathbf{k}_1'=\mathbf{K}-\mathbf{k}_1$ with $\mathbf{K}a_0=2\pi[020]$. The equivalent eigenvector will then have the components $[\boldsymbol{\Phi}_1(\mathbf{k}_1')]_\nu{}^{\xi}=[\boldsymbol{\Phi}_1(\mathbf{k}_1)]_\nu{}^{\xi}\exp(-i\mathbf{K}\cdot\boldsymbol{\varrho}_\nu)$, where the $\boldsymbol{\varrho}_\nu$ define the locations of the various sites within the unit cell of Fig. 1.)

The particular eigenvector $\boldsymbol{\Phi}_1(\mathbf{k}_1)$ shown above yields that set of spin deviations which first destabilizes the initial spiral configuration and which, therefore, most rapidly reduces the energy for values of u slightly larger than u''. The spin deviations corresponding to Eq. (21), aside from an over-all magnitude,[20] may be described as follows: Each deviation $\varkappa_{n\nu}$ ends on an ellipse $\mathcal{E}_{n\nu}$ which is centered on the tip of $\mathbf{S}_{n\nu}$ and lies in a plane perpendicular to $\mathbf{S}_{n\nu}$. The principal axes of $\mathcal{E}_{n\nu}$ lie along $\boldsymbol{\zeta}_{n\nu}$ and $\boldsymbol{\eta}_{n\nu}$, and their respective lengths are proportional to $|[\boldsymbol{\Phi}_1(\mathbf{k}_1)]_\nu{}^{\zeta}|$ and $|[\boldsymbol{\Phi}_1(\mathbf{k}_1)]_\nu{}^{\eta}|$. The angle between the deviation $\varkappa_{n\nu}$ and $\boldsymbol{\zeta}_{n\nu}$ varies as a plane wave propagating in the $\mathbf{k}_1$ direction, and the resulting configuration is illustrated in Fig. 6 for one of the sublattices. It should be noted that this configuration is ordered, notwithstanding its complexity, in the sense that a precisely-defined, long-range correlation exists amongst the various spins. Furthermore, if the [110] spiral should be the

[18] By comparison of Eq. (15) above with Eq. (14) of reference 11.

[19] To verify the existence of such states, note that the [110] spiral is degenerate with similar, locally stable spirals with k vectors in equivalent directions ([1$\bar{1}$0], [101], etc.). In other words, the energy expressed as a function of all the spin vectors has local minima at a number of different points in the spin-space, these points corresponding to the same value of the energy. Now imagine the crystal to be continuously distorted from cubic symmetry. Since such a distortion can be represented by a continuous variation of the exchange parameters, the energy function will still have local minima at points that are close to the minimum points for the cubic case for small distortions. But the arbitrariness of the distortion makes it clear that some of the local minima will possess higher energy than others, the higher ones being metastable.

[20] We have not calculated the absolute magnitude of the deviations which approximately minimizes the energy for small, positive values of $u-u''$. Such a computation would involve fourth-order terms in the energy and would be far more complicated in this case than in reference 10.

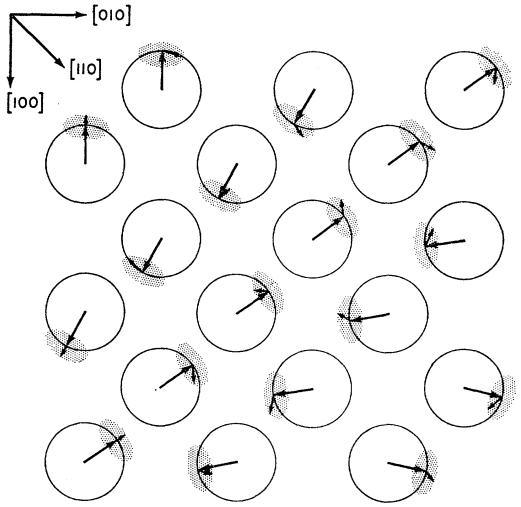

FIG. 6. Schematic illustration of the mode which destabilizes the [110] magnetic spiral at $u=u''$, drawn for one of the spinel sublattices. The cone axis has been taken to lie along the [001] direction, so that the (001) plane shown above contains the x and y components of the initial spin vectors. The short arrows indicate the projections of the small deviations and their associated ellipses upon the (001) plane, since actually these ellipses lie in planes perpendicular to the initial spins. For the purpose of illustration, the size of these ellipses has been greatly exaggerated.

true ground state for $u<u''$, then perturbation theory[10] suggests that the complicated configuration described above would be the ground state for u slightly larger than u''.

IV. IMPLICATIONS REGARDING INVARIANCE POSTULATES

As discussed in Appendix I, there is no *a priori* reason to expect any of the symmetry of a crystal lattice to be reflected in a spin configuration which minimizes the exchange energy. Nevertheless, one is tempted to speculate that the particular nature of such spin problems might cause the crystal symmetry to show up in the classical ground state in some simple form, in accordance with existing inductive evidence. For example, in any Bravais lattice the ground state is always a spiral[11]; hence Bertaut's[21] equal-relative-angle hypothesis $[\mathbf{S}(\mathbf{R})\cdot\mathbf{S}(\mathbf{R}')$ is a function only of $\mathbf{R}-\mathbf{R}']$ is invariably true in this large class of problems. A generalization for more complex structures is

$$\mathbf{S}_{n\nu}\cdot\mathbf{S}_{m\mu}=f_{\nu\mu}'(\mathbf{R}_{m\mu}-\mathbf{R}_{n\nu})=f_{\nu\mu}(\mathbf{R}_m-\mathbf{R}_n), \quad (22)$$

i.e., the angle between a pair of spins is a function only of the types of sites (ν and μ) and the vector connecting the corresponding sites, this angle being independent of the location of a spin of one type within its own sublattice. Then the inductive evidence is even more imposing, since in *every* case where the ground state of the classical Heisenberg energy has been found rigorously,[22] the equal-angle condition expressed by Eq. (22) is always satisfied for at least one of the various degenerate ground states, and usually for all of them. We shall now show that for some u values, the ground state does *not* satisfy the invariance property (22).

By means of the GLT method, our [110] magnetic spiral can be proven to be the best equal-relative-angle configuration for $u<u'$. This proof requires the result of Appendix V, where it is shown that all configurations which satisfy Eq. (22) can be written in the form

$$\mathbf{S}_{n\nu}=\mathbf{Q}_\nu(\mathbf{k})\exp(i\mathbf{k}\cdot\mathbf{R}_{n\nu})+\mathbf{Q}_\nu^*(\mathbf{k})\exp(-i\mathbf{k}\cdot\mathbf{R}_{n\nu}) +\sum_{\boldsymbol{\kappa}}\mathbf{Q}_\nu(\boldsymbol{\kappa})\exp(i\boldsymbol{\kappa}\cdot\mathbf{R}_{n\nu}), \quad (23)$$

where $\boldsymbol{\kappa}=\frac{1}{2}\mathbf{K}$ and $\mathbf{k}$ is "ordinary" (i.e., not a $\boldsymbol{\kappa}$). In other words, every such configuration contains at most one ordinary $\mathbf{k}$, plus $\boldsymbol{\kappa}$'s, the class of ferrimagnetic spirals being a special case with $\mathbf{Q}_\nu(\boldsymbol{\kappa})=0$ for $\boldsymbol{\kappa}\neq 0$.

As seen in Sec. II(B), the GLT method guarantees that our [110] spiral has a lower energy than any configuration constructed from Fourier components with $\mathbf{k}$'s drawn exclusively from the "good" set. Investigation of this "good" set shows it to contain all the $\boldsymbol{\kappa}$'s for values of u at least as large as u', as well as some cubic equivalent of every $\mathbf{k}$ for $u<u'$. Since any cubic symmetry operation leaves the energy invariant and carries one $\boldsymbol{\kappa}$ into another $\boldsymbol{\kappa}$, it follows that any configuration given by Eq. (23) must be degenerate with some cubically equivalent configuration having Fourier components drawn exclusively from the "good" set when $u<u'$. Therefore our [110] magnetic spiral yields the lowest energy of any configuration which satisfies the equal-relative-angle condition of Eq. (22) for $u<u'$.

However, in Sec. III we found the [110] spiral to be locally unstable, and consequently not the ground state, if $u>u''$. From this fact together with the result of the preceding paragraphs, it follows that Eq. (22) cannot be satisfied in the ground state for $u''<u<u'$. *Thus there must exist ground-state spin configurations where, for some* $n\nu$, $m\mu$, *and* p,

$$\mathbf{S}(\mathbf{R}_{n\nu})\cdot\mathbf{S}(\mathbf{R}_{m\mu})\neq\mathbf{S}(\mathbf{R}_{n\nu}+\mathbf{R}_p)\cdot\mathbf{S}(\mathbf{R}_{m\mu}+\mathbf{R}_p). \quad (24)$$

Although our proof holds only for $u<u'$, Eq. (24) will probably be valid over a larger range of u. Furthermore, there is no doubt that Eq. (24) will hold over a class of distorted spinels, since continuous distortions can be represented by continuous changes in the interaction parameters and the minimum-energy spin configuration can be chosen to be a continuous function of these parameters.[23]

[21] The hypothesis U in reference 14.

[22] We list these cases: (A) Arbitrary J_{ij}. All Bravais lattices (reference 11), corundum structure [N. Menyuk, Quarterly Progress Report on Solid State Research, Lincoln Laboratory, M.I.T., July 15, 1961, p. 59, ASTIA 262282], and hexagonal-close-packed structure [T. A. Kaplan, Phys. Rev. **124**, 329 (1961)]. (B) Restricted J_{ij}. *ABAB* linear chain (references 11 and 39), tetragonally distorted spinels (reference 9), and cubic spinels with nonmagnetic A sites [T. A. Kaplan, Massachusetts Institute of Technology Lincoln Laboratory Group Report 53G-0036, 1960 (unpublished)].

[23] Since any distortion from cubic symmetry will lower that symmetry, and hence will not increase the degeneracy.

In Appendix I it is shown that a classical ground state need not satisfy invariance conditions; the counterexample given above goes further in that it proves the attractive equal-relative-angle hypothesis *not* to be generally valid. Other invariance postulates have been introduced in the literature, as discussed in Appendix V, but the intractability of the enumeration of all the corresponding spin configurations prohibits any similar treatment. Nevertheless, the failure of one of them casts doubt on the others, and this doubt is strengthened by the existence of a counterexample to the Gersch-Koehler condition[13] for the case of an Ising linear chain, where the configurations can be enumerated.[24]

V. NEUTRON DIFFRACTION

A. General Considerations

The underlying purpose of our attempt to find the theoretical ground state of the classical Heisenberg energy is to provide the necessary connecting link between experiment and the fundamental theory. Traditionally, the approach of the experimental diffractionist has been based on the assumption that the spin configuration will reflect much of the symmetry of the crystal lattice. However, as discussed in Appendix I and Sec. IV, the crystal symmetry implies nothing about the spin symmetry. In general, the spin system will possess no symmetry in the conventional sense, the configurations of Secs. II and III being good examples. As shown below, the Fourier components of such configurations yield the most convenient description of the resulting neutron diffraction.

Neutrons are scattered both by nuclear and magnetic forces. However, Halpern and Johnson have shown[25] that the resulting intensities are purely additive when the neutrons are unpolarized. It follows from the above treatment, that the magnetic contribution to the intensity of unpolarized neutrons elastically scattered from a single crystal is proportional to

$$\sigma(\mathbf{e})=|\mathbf{P}(\mathbf{e})|^2-|\hat{e}\cdot\mathbf{P}(\mathbf{e})|^2, \tag{25}$$

where $\mathbf{e}$ is the neutron scattering vector (difference between the scattered and incident neutron wave vectors), $\hat{e}$ is a unit vector in the direction of $\mathbf{e}$, and

$$\mathbf{P}(\mathbf{e})=\sum_{n,\nu} S_\nu f_\nu(\mathbf{e})\mathbf{S}_{n\nu}\exp(i\mathbf{e}\cdot\mathbf{R}_{n\nu}), \tag{26}$$

$f_\nu(\mathbf{e})$ being the form factor which describes the effect of the distribution of electrons around an ionic core.[26,27]

This result can be derived simply from the work of Corliss, Hastings, and Brockman[28] by writing $\mathbf{q}_{n\nu}=\hat{e}(\hat{e}\cdot\mathbf{S}_{n\nu})-\mathbf{S}_{n\nu}$, and thereby removing their sublattice assumption.

The cross section $\sigma(\mathbf{e})$ differs from the "structure factor" of reference 28 by a numerical factor and by the necessary inclusion of the summation over all the unit cells in a crystallite. To eliminate this summation, we note that any arbitrary spin configuration can be written in terms of its Fourier components,

$$\mathbf{S}_{n\nu}=\sum_{\mathbf{k}}\mathbf{Q}_\nu(\mathbf{k})\exp(i\mathbf{k}\cdot\mathbf{R}_{n\nu}). \tag{27}$$

Since $\mathbf{R}_{n\nu}=\mathbf{R}_n+\boldsymbol{\varrho}_\nu$, it follows that

$$\mathbf{P}(\mathbf{e})=\sum_{\mathbf{k},\nu} f_\nu(\mathbf{e})S_\nu\mathbf{Q}_\nu(\mathbf{k})\exp[i(\mathbf{k}+\mathbf{e})\cdot\boldsymbol{\varrho}_\nu]\times\sum_n\exp[i(\mathbf{k}+\mathbf{e})\cdot\mathbf{R}_n]. \tag{28}$$

Here the summation over n is the familiar interference function consisting of essentially delta-function peaks whenever $\mathbf{k}+\mathbf{e}-\mathbf{K}=0$, $\mathbf{K}$ being any reciprocal-lattice vector. Hence we write

$$\mathbf{P}(\mathbf{e})=\sum_{\mathbf{K},\mathbf{k}} D(\mathbf{k}+\mathbf{e}-\mathbf{K})\mathbf{F}(\mathbf{K},\mathbf{k}), \tag{29}$$

where the structure factor is given by

$$\mathbf{F}(\mathbf{K},\mathbf{k})=\sum_\nu f_\nu(\mathbf{K}-\mathbf{k})S_\nu\mathbf{Q}_\nu(\mathbf{k})\exp(i\mathbf{K}\cdot\boldsymbol{\varrho}_\nu), \tag{30}$$

and where $D(\mathbf{h})$ is sharply peaked at $\mathbf{h}=0$.

The foregoing equations show that the scattered neutron intensity can be appreciable only when $\mathbf{e}=\mathbf{K}-\mathbf{k}$, where $\mathbf{k}$ must be a wave vector associated with a nonvanishing component in the Fourier expansion of $\mathbf{S}_{n\nu}$ [i.e., $\mathbf{Q}_\nu(\mathbf{k})\neq 0$ for some ν].

---

[24] T. A. Kaplan and D. H. Lyons (to be published).

[25] O. Halpern and M. H. Johnson, Phys. Rev. **55**, 898 (1939).

[26] The standard theory by means of which neutron diffraction experiments are interpreted involves Eq. (25), in which the symbol $\mathbf{S}_n$ represents the quantum-mechanical average value $\langle 0|\mathbf{S}_n|0\rangle$ of the nth spin in the ground state (we are considering only $T=0$). One can obtain Eq. (25) with this definition of $\mathbf{S}_n$ by omitting all terms in the Halpern-Johnson result that involve transitions from one state of the crystal to a different one ("inelastic" terms). However, because the crystal is macroscopic and, therefore, has densely-spaced levels (with spacing much smaller than the experimental energy resolution as well as the incident neutron energy), it is not reasonable to omit the inelastic terms. It is more reasonable to expect that the contribution of all the terms in the Halpern-Johnson formula to the intensity in a Bragg peak is given by the static approximation [see L. Van Hove, Phys. Rev. **95**, 1374 (1954)] as in the case of X rays, since the Bragg peak involves only energy changes much smaller than the incident neutron energy. The use of the static approximation is equivalent to replacing the products of the average spins $\langle 0|\mathbf{S}_n|0\rangle\langle 0|\mathbf{S}_m|0\rangle$ (as occur in Eq. (25) if the $\mathbf{S}_n$ are interpreted as $\langle 0|\mathbf{S}_n|0\rangle$) by the average of the products $\langle 0|\mathbf{S}_n\mathbf{S}_m|0\rangle$.

Although this static approximation involves a negligible change in the predicted intensity for a Bragg peak when one uses either the spin wave or the molecular field approximations, the use of the average of the product in the cross section would obviate the difficulty which arises in the exact quantum-mechanical theory of antiferromagnetism; in this case $\langle 0|\mathbf{S}_n|0\rangle=0$ for the exact ground state, but of course $\langle 0|\mathbf{S}_n\mathbf{S}_m|0\rangle$ is not zero. A similar difficulty arises in the case of spirals where, for example, the average values $\langle 0|\mathbf{S}_n|0\rangle$ would not look like a ferrimagnetic spiral because of the translational invariance of the exact quantum-mechanical ground state; again the use of the static approximation would remove the difficulty.

Furthermore, it may be shown that Eq. (25), for large N, depends on the $\mathbf{S}_n$ only through the correlation function $\Gamma_m=N^{-1}\Sigma_n\mathbf{S}_n\mathbf{S}_{n+m}$. That is, the neutrons "see" the spin system via Eq. (25) only through the spacial average Γ_m of the products $\mathbf{S}_n\mathbf{S}_{n+m}$. Regarding the $\mathbf{S}_n$ as classical variables, this correlation function (for $\mathbf{R}_m$ within a domain) will be the same as the classical ensemble average $\langle\mathbf{S}_n\mathbf{S}_{n+m}\rangle_c$ (averaged over the degenerate states at $T=0$). Therefore, in this classical picture, the standard use of Eq. (25) amounts to the assumption of the static approximation.

[27] These expressions for the cross section have also been used recently by W. C. Koehler [Acta Cryst. **14**, 535 (1961)] to derive the intensity associated with spirals in Bravais lattices.

[28] L. M. Corliss, J. M. Hastings, and F. G. Brockman, Phys. Rev. **90**, 1013 (1953).

Thus, associated with each point $\mathbf{K}$ in reciprocal space there is a number of scattering points, $\mathbf{K}-\mathbf{k}$, equal to the number of different $\mathbf{k}$'s for which there are nonzero Fourier components of the spins. The $\mathbf{k}=0$ Fourier component produces magnetic peaks only at the nuclear peak locations ($\mathbf{e}=\mathbf{K}$). The peaks arising from $\mathbf{k}=0$ will be called "fundamentals," and all others will be called "satellites." It should be emphasized that the fundamentals are not necessarily larger than the satellites; for example, in the case of simple spirals $\mathbf{Q}_\nu(0)=0$, so that all the scattering is through the satellites. We also point out that since all antiferromagnetic spin configurations observed before the advent of spirals are just particular cases of simple spirals, each involving one special k vector, their diffraction pattern can be described conveniently in the above language (all the peaks being satellites in Bravais lattices). Such a description has an advantage over the conventional method of reindexing the peaks on a new unit cell, since it does not suffer from the drastic discontinuity that occurs in the conventional method when the k vector changes slightly from such special values.

For the general magnetic spiral defined by Eq. (9), the only nonzero Fourier components are $Q_\nu{}^{z'}(0)$ and $Q_\nu{}^{y'}(k_0)=-iQ_\nu{}^{x'}(k_0)$. Consequently, Eq. (30) gives

$$\begin{aligned}&\mathbf{F}(\mathbf{K},0)=\hat{z}'F^{z'}(\mathbf{K},0)=\hat{z}'F(\mathbf{K},0),\\&\mathbf{F}(\mathbf{K},\mathbf{k}_0)=(\hat{x}'-i\hat{y}')F^{x'}(\mathbf{K},\mathbf{k}_0)=(\hat{x}'-i\hat{y}')F(\mathbf{K},\mathbf{k}_0).\end{aligned}\tag{31}$$

Then the explicit evaluation of the sum over $\mathbf{k}$ in Eq. (29) yields

$$\begin{aligned}\mathbf{P}(\mathbf{e})=\hat{z}'\textstyle\sum_{\mathbf{K}}D(\mathbf{e}-\mathbf{K})F(\mathbf{K},0)+(\hat{x}'-i\hat{y}')\\\times\textstyle\sum_{\mathbf{K}}[D(\mathbf{e}+\mathbf{k}_0-\mathbf{K})F(\mathbf{K},\mathbf{k}_0)\\+D(\mathbf{e}-\mathbf{k}_0-\mathbf{K})F(\mathbf{K},-\mathbf{k}_0)].\end{aligned}\tag{32}$$

Provided that $\mathbf{k}_0$ is not equal to half of a reciprocal-lattice vector, $D(\mathbf{e}+\mathbf{k}_0-\mathbf{K})$ and $D(\mathbf{e}-\mathbf{k}_0-\mathbf{K}')$ cannot simultaneously be nonzero for a given $\mathbf{e}$. Then the magnetic cross section of Eq. (25) becomes

$$\begin{aligned}\sigma(\mathbf{e})=[1-(\hat{e}\cdot\hat{z}')^2]\textstyle\sum_{\mathbf{K}}D^2(\mathbf{e}-\mathbf{K})|F(\mathbf{K},0)|^2\\+[1+(\hat{e}\cdot\hat{z}')^2]\textstyle\sum_{\mathbf{K}}[D^2(\mathbf{e}+\mathbf{k}_0-\mathbf{K})|F(\mathbf{K},\mathbf{k}_0)|^2\\+D^2(\mathbf{e}-\mathbf{k}_0-\mathbf{K})|F(\mathbf{K},-\mathbf{k}_0)|^2].\end{aligned}\tag{33}$$

Recalling that $\hat{z}'$ is the direction of the cone axis and, hence, of the net magnetic moment, we see from Eq. (33) that the application of an external magnetic field along the scattering vector $\mathbf{e}$ will reduce the intensity of the fundamentals ($\mathbf{e}=\mathbf{K}$), while increasing the intensities of the satellites ($\mathbf{e}=\mathbf{K}\pm\mathbf{k}_0$).

In the case of diffraction from polycrystalline samples, one must average (33) over all crystal orientations. There are two aspects of such an averaging process in the presence of spirals which are different from the more familiar cases, and which enter in a significant way to the intensity calculations. One of these is the fact that in general the direction of the cone axis $\hat{z}'$ will be correlated with the propagation vector $\mathbf{k}_0$, due to anisotropy forces; hence one must calculate the diffraction pattern for a given $\hat{z}'$ relative to $\mathbf{k}_0$ and to the crystal axes, instead of replacing $(\hat{e}\cdot\hat{z}')^2$ by an average value. The other arises from the higher probability of having more than one scattering point contribute to a given powder peak (a satellite of one $\mathbf{K}$ might contribute at the same scattering angle as a fundamental at a different $\mathbf{K}$, etc.). Given the experimental data, the existence of such coinciding contributions can cause serious difficulty in the construction of a suitable spin configuration.

B. Details for a Normal Cubic Spinel

The neutron diffraction pattern calculated for our [110] magnetic spiral exemplifies the general properties discussed above. For one, single-domain crystallite, there are associated with each reciprocal lattice point $\mathbf{K}$ three scattering points, $\mathbf{K}+\mathbf{k}_0$, $\mathbf{K}-\mathbf{k}_0$ (the satellites), and $\mathbf{K}$ (the fundamental). However, for the value of $\mathbf{k}_0$ computed in Sec. II(A), the magnetic scattering from the following pairs of scattering points coincide in the resulting powder diffraction pattern: $(220)-\mathbf{k}_0$ and (002), $(222)-\mathbf{k}_0$ and (220), $(202)+\mathbf{k}_0$ and (113), (400) $-\mathbf{k}_0$ and (222), and $(2\bar{2}2)+\mathbf{k}_0$ and $(330)-\mathbf{k}_0$.

Once the positions of possible diffraction peaks have been determined, the next step is the explicit evaluation of the corresponding structure factors. Because of the pairing of the sublattices ($\nu=1$ and 2, 3 and 4, 5 and 6) which occurs in our [110] spiral, the structure factors $F(\mathbf{K},0)$, $F(\mathbf{K},\mathbf{k}_0)$, and $F(\mathbf{K},-\mathbf{k}_0)$ all vanish identically for $\pm\mathbf{K}a_0/2\pi=(200)$, (020), (420), (240), (204), (024), etc. In addition, calculations based on the spiral parameters of Fig. 2, with values of S_ν appropriate to manganese chromite, lead to negligible structure factors[29] for the satellites $(111)\pm\mathbf{k}_0$ and $(331)\pm\mathbf{k}_0$, to very small ones for $(000)\pm\mathbf{k}_0$, and to generally small ones for many of the other scattering points in reciprocal space. Thus the predicted pattern becomes greatly simplified. In particular, the only appreciable peaks correspond to (111), $(1\bar{1}1)\pm\mathbf{k}_0$, (220) and $(222)-\mathbf{k}_0$, (400), (002) and $(220)-\mathbf{k}_0$, $(002)\pm\mathbf{k}_0$, (222) and $(400)-\mathbf{k}_0$, (113) and $(202)+\mathbf{k}_0$, $(113)-\mathbf{k}_0$, $(202)-\mathbf{k}_0$, and $(113)+\mathbf{k}_0$, arranged approximately according to decreasing intensity. Half of the above peaks occur at the nuclear positions, so that only a few "extra" peaks are to be expected.

If u is slightly greater than u'', the [110] spiral is unstable with respect to a certain mode of small spin deviations, as described in Sec. III. As given in Appendix IV, the resulting deviated spins possess several additional nonzero Fourier components, corresponding to six more k vectors, so that there will be six additional scattering points associated with each reciprocal-lattice point. Obviously, the resulting neutron diffraction pattern will be much more complicated than that of the magnetic spiral.

[29] Here we employed the standard approximation of using the same form factor for all the ions.

When the deviations are sufficiently small, the diffraction peaks arising from the [110] spiral will remain essentially unaltered and some small, additional peaks will appear because of the deviations. The relative intensities among these additional peaks can be calculated in a straightforward manner from Eqs. (21), (D8), (25), (29), and (30), together with the spiral parameters of Fig. 2 and the definition of the $\zeta_{n\nu}$, $\eta_{n\nu}$ coordinate systems. Such a calculation shows that the largest of these additional peaks lies approximately midway between the (000)$+\mathbf{k}_0$ satellite and the (111) fundamental.

VI. COMPARISON WITH EXPERIMENT

A. The Ground State (4.2°K)

Experimental results could be used to test the validity of the classical Heisenberg approximation if the theoretical ground state were known. Despite our failure to rigorously determine the ground state, much information can be gained by comparing our calculated neutron diffraction patterns with those obtained from experiment. In particular, an examination of the similarities and discrepancies between the observed and theoretical properties of manganese chromite (to date, the only normal cubic spinel with a non-Néel spin configuration which has been carefully investigated[1]) leads to several important conclusions. The discussion below illustrates how the configurations given in Secs. II and III can facilitate the interpretation of observed neutron patterns on the one hand, and on the other, how the experimental *a posteriori* knowledge of the actual ground state can serve to illuminate the theoretical approach.

We used a vibrating-coil magnetometer[30] to measure the spontaneous magnetization of a polycrystalline sample of pure[31] manganese chromite, and our value of about 1.2 μ_B per molecule is in agreement with Jacobs' previous findings.[32] Calculation of the theoretical dependence of the net moment upon u from the spiral parameters of Fig. 2 shows that the smallest value of u consistent with the measured magnetization must lie between 1.50 and 1.75 when reasonable moments are assigned to the Mn^{++} ions. In the present context, the significance of this result is that u must be greater than u'', so that the [110] magnetic spiral cannot be the ground state.

Corliss and Hastings[1] have recently investigated the above sample of $MnCr_2O_4$ by neutron diffraction, and we refer the reader to their paper for a quantitative comparison between theory and experiment. However, we wish to discuss here the over-all qualitative agreement between their experimental findings and the pattern expected from our [110] spiral for $u\cong 1.6$. The magnetic contributions to the experimental diffraction pattern at 4.2°K consist not only of fundamental peaks at the nuclear positions, but also of several large "extra" peaks whose locations agree strikingly with the satellite positions calculated from the $\mathbf{k}_0$ computed for our [110] magnetic spiral. In addition, there is qualitative agreement in the intensities, which can be summarized as follows: None of the theoretical peaks with negligible predicted intensities were observed, all of the peaks with large predicted intensities were observed to be large, and there were no other large magnetic peaks in the experimental pattern. Furthermore, there were a number of small peaks ($<10\%$ of the largest satellite) found experimentally which are predicted in the right order of magnitude as well as in the right locations. Finally, an external magnetic field applied along the scattering vector caused the fundamentals to decrease in intensity and the satellites to increase, as expected for a ferrimagnetic spiral [see Sec. V(A)].

In addition to the above agreement with a spiral model, there are important discrepancies. The observed diffraction pattern included two small "additional" peaks which do not arise from the ferrimagnetic spiral, and the fundamental peaks were all smaller than those predicted for the spiral, although the predicted satellite intensities give fair agreement.[1] A consideration of all of the above aspects of the experimental results strongly suggests that the actual low-temperature spin configuration in $MnCr_2O_4$ is almost, though not quite, a ferrimagnetic spiral, in the sense that its principal Fourier components are given approximately by our [110] magnetic spiral.

In order to appreciate the significance of this conclusion, it is necessary to recall the logical structure of our theory. To begin with, we assumed that the classical Heisenberg theory with only nearest-neighbor *A-B* and *B-B* interactions would give a reasonable first approximation to the actual spin ordering in manganese chromite (or any normal cubic spinel). Then we constructed a [110] magnetic spiral, and showed that it satisfies several stringent conditions upon possible ground-state spin configurations, leading us to believe that this spiral probably is the ground state for $u<u''\cong 1.3$. For $u>u''$, the spiral is definitely not the ground state. Nevertheless, we may consider it here to be an approximation in the variational sense.

In the above spirit, we used the measured magnetic moment to determine our single adjustable parameter u, obtaining $u\cong 1.6$ and thereby fixing all the remaining spiral parameters (wavelength, cone angles, and phases). Upon further comparison with the diffraction results, the calculated spiral showed a striking qualitative agreement. Moreover, the existence of real discrepancies is in accord with our result that the spiral cannot be the ground state for $u\cong 1.6$. Thus the experimental result agrees with the conclusion of our chain of reasoning. Keeping in mind the considerable complexity of the diffraction pattern, and the fact that our theory contains only one adjustable parameter u which determines

[30] K. Dwight, N. Menyuk, and D. Smith, J. Appl. Phys. **29**, 491 (1958).
[31] E. Whipple and A. Wold, J. Phys. Chem. Solids (to be published).
[32] I. S. Jacobs, J. Phys. Chem. Solids **15**, 54 (1960).

the best over an enormous variety of spin configurations, it is quite reasonable to conclude that this agreement is not fortuitous. Hence, the comparison with experiment supports the entire logical structure, including our basic assumption, and suggests that the exact theoretical ground state in our model for $u \cong 1.6$ does not differ greatly from our spiral.

If this difference were sufficiently small, then the deviational mode calculated in Sec. III should improve the agreement between theory and experiment. However, this is not the case, since the largest of the peaks expected from the destabilizing mode [Sec. V(B)] is absent from the experimental pattern. One possible explanation for this discrepancy is that $\Delta u = 1.6 - u''$ might not be sufficiently small in the sense of the convergence of perturbation theory, so that higher order terms might be very important. Another possibility is that our model neglects some important interactions. The latter view is given credence by the fact that the experimental diffraction pattern for zinc chromite[33] evidences a long-range ordering of the spins, which, together with Anderson's result,[34] strongly suggests the existence of next-nearest-neighbor *B-B* interactions.[35] Furthermore, it is possible that the rather high sensitivity of spiral-like configurations to impurities[1] could be a contributory factor.

B. Temperature Dependence

In Appendix VI, the spin configuration appropriate to the Curie (or Néel) temperature is calculated in the molecular field approximation. Knowing u, one can reasonably infer the qualitative temperature dependence of the spin configuration of a normal cubic spinel from the results of Appendix VI. For example, upon decreasing the temperature of a material with $u = 1.6$, it will first become ferrimagnetic with a Néel-type configuration where $\langle \mathbf{S}_{n\nu} \rangle$ are all collinear. At a lower temperature, the spin configuration will change to a [110] magnetic spiral which, at a still lower temperature, will become unstable with respect to some particular mode of small spin deviations, resulting in a more complicated ground state. The transition from the Néel-type to spiral configurations has been observed in manganese chromite.[1] The onset of the deviational mode, besides being difficult to define, would occur at an experimentally awkward temperature in manganese chromite, so that it is not surprising that it has not been observed. Thus, the temperature dependence yields additional qualitative agreement between our results and the experimental findings.

[33] L. Corliss and J. Hastings (private communication).
[34] P. W. Anderson, Phys. Rev. **102**, 1008 (1956).
[35] An investigation of these interactions by means of theoretical approach similar to the present one, but for the case of nonmagnetic *A* sites, has been initiated by one of us (K.D.).

VII. SUMMARY

We have assumed that the classical Heisenberg energy with only nearest-neighbor *A-B* and *B-B* interactions will give a satisfactory description of the magnetic properties of normal cubic spinels. By using the GLT method in an attempt to minimize this energy function of many ($\approx 10^{23}$) variables, we have obtained a spin configuration which is of lower energy than any previously obtained whenever the Néel state is unstable (i.e., $u > 8/9$). This configuration is a ferrimagnetic spiral with its propagation vector in the [110] direction; the remaining parameters (cone angles, etc.) are given as explicit functions of the single exchange parameter u.

The above spiral is probably the ground state for $8/9 \leqslant u < 1.298$. This conclusion is suggested by the following properties which are proven rigorously for this range of u: The spiral has lower energy than any neighboring configuration (i.e., it is locally stable); and it is the lowest over an additional large class of configurations, which includes all ferrimagnetic spirals, all equal-relative-angle configurations, and many others. However, it should be realized that these results do not constitute a rigorous proof that the spiral is the ground state for this range of u.

The spiral is definitely not the ground state for $u > 1.298$, since here it is found to be locally unstable. Furthermore, we prove that, for a finite range of u in this instability region, the ground state must be a more complicated configuration in which the angles between spins are not translationally invariant.

Our general theoretical approach is supported by a consideration of the experimental data for manganese chromite. This support arises from the striking similarities between the complicated neutron diffraction pattern observed by Corliss and Hastings[1] and that predicted by our spiral model. Moreover, since this model gives $u \cong 1.6$ for manganese chromite, the agreement suggests that our ferrimagnetic spiral is a good approximation to the actual ground state even for values of u appreciably greater than 1.298.

ACKNOWLEDGMENTS

We should like to thank L. Corliss and J. Hastings for many discussions of their unpublished neutron diffraction experiments, and A. Wold for discussions concerning the chemistry of cubic spinels. We are pleased to acknowledge the help of Mrs. Ann Sherman on all aspects of our work involving the use of the IBM 709 computer. Finally, we wish to express our appreciation for the encouragement of J. B. Goodenough throughout the entire course of this research.

APPENDIX I. SYMMETRY

Since various usages of terms relating to symmetry have occurred in the literature, a statement of our defi-

nitions seems desirable. We are concerned in this paper with the minimization of a function in which spin vectors are the unknown variables and exchange interactions are the parameters. In general, the largest group of symmetry operations that leave the Heisenberg exchange energy of Eq. (2) invariant is the full space group of the crystal before the association of spin vectors with the lattice sites. All the operations O of this space group (*Fd3m* for a normal cubic spinel) leave the exchange interactions invariant,

$$\bar{J}(O\mathbf{R}_{n\nu},O\mathbf{R}_{m\mu})=\bar{J}(\mathbf{R}_{n\nu},\mathbf{R}_{m\mu}). \tag{A1}$$

Equation (A1) expresses the only dependence of our spin problem upon symmetry, no *a priori* assumptions about the symmetry of the *crystal with spins* being made.[36]

The translations $\mathcal{T}_n$ under which the structure is invariant are included in the above space group, and the corresponding displacements $\mathbf{R}_n$ define the Bravais lattice associated with the structure. Given any particular site, the translations $\mathcal{T}_n$ generate a complete (exhaustive) set of "equivalent" sites with positions $\mathbf{R}_{n\nu}=\mathbf{R}_n+\boldsymbol{\varrho}_\nu$, this set being called the νth sublattice. (We shall refer to a crystal as Bravais if all the magnetic ions fall on a single sublattice, and non-Bravais otherwise.) In our terminology, two sites are equivalent if and only if they are connected by a translation of the space group, and such equivalence is independent of any association of spin vectors with the sites.

Finally, it is clear that the invariance of the Heisenberg energy function with respect to specified symmetry operations does not in itself imply that a ground-state spin configuration be similarly invariant. For example, the classical ground state need not be translationally invariant nor even belong to the class of equal-relative-angle configurations (see Appendix V), for the same reason that an even function $f(x)=f(-x)$ need not attain its minimum value at $x=-x=0$. The invariance expressed by Eq. (A1) implies only that all spin configurations which are interrelated by the space group operations be degenerate.

APPENDIX II. THE MATRICES

For a cubic spinel having nearest-neighbor A-B and B-B interactions only, and with the sublattice definitions given in Fig. 1, Eqs. (4) yield the matrix

$$\frac{\mathbf{L}(\mathbf{k})}{3J_{AB}S_AS_B}=\begin{bmatrix} 0 & 0 & \eta_1 & \eta_2 & \eta_3 & \eta_4 \\ 0 & 0 & \eta_1^* & \eta_2^* & \eta_3^* & \eta_4^* \\ \eta_1^* & \eta_1 & 0 & \frac{1}{2}u\zeta_{12} & \frac{1}{2}u\zeta_{13} & \frac{1}{2}u\zeta_{14} \\ \eta_2^* & \eta_2 & \frac{1}{2}u\zeta_{12} & 0 & \frac{1}{2}u\zeta_{23} & \frac{1}{2}u\zeta_{24} \\ \eta_3^* & \eta_3 & \frac{1}{2}u\zeta_{13} & \frac{1}{2}u\zeta_{23} & 0 & \frac{1}{2}u\zeta_{34} \\ \eta_4^* & \eta_4 & \frac{1}{2}u\zeta_{14} & \frac{1}{2}u\zeta_{24} & \frac{1}{2}u\zeta_{34} & 0 \end{bmatrix}, \tag{B1}$$

where the functions η_j and ζ_{ij} are given by

$$\begin{aligned}
\eta_1&=\tfrac{1}{3}\{\exp[i\mathbf{k}\cdot(\bar{1}13)]+\exp[i\mathbf{k}\cdot(31\bar{1})]+\exp[i\mathbf{k}\cdot(131)]\},\\
\eta_2&=\tfrac{1}{3}\{\exp[i\mathbf{k}\cdot(1\bar{1}3)]+\exp[i\mathbf{k}\cdot(13\bar{1})]+\exp[i\mathbf{k}\cdot(311)]\},\\
\eta_3&=\tfrac{1}{3}\{\exp[i\mathbf{k}\cdot(11\bar{3})]+\exp[i\mathbf{k}\cdot(\bar{3}11)]+\exp[i\mathbf{k}\cdot(1\bar{3}1)]\},\\
\eta_4&=\tfrac{1}{3}\{\exp[i\mathbf{k}\cdot(113)]+\exp[i\mathbf{k}\cdot(\bar{1}31)]+\exp[i\mathbf{k}\cdot(3\bar{1}1)]\},\\
\zeta_{12}&=\cos[\mathbf{k}\cdot(\bar{2}20)],\quad \zeta_{23}=\cos[\mathbf{k}\cdot(022)],\\
\zeta_{13}&=\cos[\mathbf{k}\cdot(\bar{2}02)],\quad \zeta_{24}=\cos[\mathbf{k}\cdot(20\bar{2})],\\
\zeta_{14}&=\cos[\mathbf{k}\cdot(02\bar{2})],\quad \zeta_{34}=\cos[\mathbf{k}\cdot(220)],
\end{aligned} \tag{B2}$$

with the notation $(hkl)=\frac{1}{8}a_0(h\hat{x}+k\hat{y}+l\hat{z})$.

For $\mathbf{k}$ in the [110] direction, the above matrix can be written explicitly as

$$\frac{\mathbf{L}(k[110]/\sqrt{2})}{3J_{AB}S_AS_B}=\begin{bmatrix} 0 & 0 & \eta' & \eta' & \eta & \eta^* \\ 0 & 0 & \eta' & \eta' & \eta^* & \eta \\ \eta' & \eta' & 0 & \frac{1}{2}u & \frac{1}{2}u\zeta & \frac{1}{2}u\zeta \\ \eta' & \eta' & \frac{1}{2}u & 0 & \frac{1}{2}u\zeta & \frac{1}{2}u\zeta \\ \eta^* & \eta & \frac{1}{2}u\zeta & \frac{1}{2}u\zeta & 0 & \frac{1}{2}u\zeta' \\ \eta & \eta^* & \frac{1}{2}u\zeta & \frac{1}{2}u\zeta & \frac{1}{2}u\zeta' & 0 \end{bmatrix}, \tag{B3}$$

where

$$\begin{aligned}
\eta&=\cos\rho-(i/3)\sin\rho,\\
\eta'&=1-(4/3)\sin^2\rho,\\
\zeta&=\cos\rho,\\
\zeta'&=\cos 2\rho,
\end{aligned} \tag{B4}$$

with $\rho=(ka_0)/(4\sqrt{2})$. This matrix can be partially diagonalized by transforming it from the sublattice basis used above into a new basis defined by the following linear combinations of the sublattice basis vectors:

$$\begin{aligned}
\psi_1&=(1/\sqrt{2})(0,0,1,-1,0,0),\\
\psi_2&=(1/\sqrt{2})(1,-1,0,0,0,0),\\
\psi_3&=(1/\sqrt{2})(0,0,0,0,1,-1),\\
\psi_4&=(1/\sqrt{2})(1,1,0,0,0,0),\\
\psi_5&=(1/\sqrt{2})(0,0,1,1,0,0),\\
\psi_6&=(1/\sqrt{2})(0,0,0,0,1,1).
\end{aligned} \tag{B5}$$

The matrix elements in this new basis are defined by

$$L_{\nu\mu}'(k[110]/\sqrt{2})=(\psi_\nu,\mathbf{L}(k[110]/\sqrt{2})\psi_\mu), \tag{B6}$$

[36] The other approach to the problem of spin configurations would be to take certain symmetry properties of the *crystal with spins included* as known from experiment, and investigate only the class of configurations consistent with these properties. This approach has been successful in simple cases, but in more complicated cases the magnetic symmetry is so low that little can be learned about the existing spin configuration from this approach. Furthermore, this approach avoids the important fundamental problem of determining if the classical Heisenberg theory yields a valid approximation to the magnetic properties.

and the resulting matrix consists of 1×1, 2×2, and 3×3 submatrices along the diagonal, these submatrices corresponding to ψ_1; ψ_2 and ψ_3; and ψ_4, ψ_5, and ψ_6. The behavior of the matrix $\mathfrak{L}$, related to $\mathbf{L}$ by Eqs. (3) and (7), is completely analogous.

Both λ_0 and $\lambda_1(\mathbf{k}_0)$ arise from the 3×3 submatrix. Hence both of the corresponding eigenvectors will have the general form

$$\Psi(\mathbf{k})=a(\mathbf{k})\psi_4+b(\mathbf{k})\psi_5+c(\mathbf{k})\psi_6 = (1/\sqrt{2})(a,a,b,b,c,c). \quad \text{(B7)}$$

The right-hand side of Eq. (B7) explicitly gives the components of $\Psi(\mathbf{k})$ in the sublattice basis, and the multiplication of these components by suitable numbers $a^u(\mathbf{k})$ gives $P_\nu{}^u(\mathbf{k})$ $(u=x', y', z')$ which define[11] the corresponding spin configuration according to

$$S_{n\nu}{}^u=\sum_{\mathbf{k}}\beta_\nu P_\nu{}^u(\mathbf{k})\exp(i\mathbf{k}\cdot\mathbf{R}_{n\nu}). \quad \text{(B8)}$$

APPENDIX III. THE SOLUTION

The solution of the simultaneous equations described in Sec. II(A) can be reduced to the following computational procedure, valid for the region $u_0\leqslant u\leqslant 2$. First a value is chosen for k. Then, with $\rho=ka_0/4\sqrt{2}$, one can evaluate:

$$h=1-4\sin^2\rho; \quad \text{(C1)}$$

$$A=h^2(h+1)/16,$$
$$B=h(h^3+9h^2+21h+5)/18, \quad \text{(C2)}$$
$$C=-4(2h^2+11h+17)/9;$$

$$\mu^2=(-B+[B^2-4AC]^{\frac{1}{2}})/2A,$$
$$\mu'^2=\mu^2h[\mu^2h(h-1)-16]/[\mu^2h(h+3)+16h+32]; \quad \text{(C3)}$$

$$\alpha=(8+\mu^2h)/2\,\mu(1+h),$$
$$\alpha'=(\mu^2h-4\,\mu'\alpha)/4\,\mu'; \quad \text{(C4)}$$

$$\tau=(h+3)^{\frac{1}{2}}(8h+16+3\,\mu^2h)/2\,\mu(h^2+4h+7),$$
$$\tau'=3[\mu^2h-2\,\mu\tau(h+3)^{\frac{1}{2}}]/4\,\mu'(h+2); \quad \text{(C5)}$$

$$u^2=\mu^2\mu'^2(\alpha^2\tau'^2-\alpha'^2\tau^2)/[\mu'^2(\tau'^2-\alpha'^2)-\mu^2(\tau^2-\alpha^2)]; \quad \text{(C6)}$$

$$\beta=\mu/u \quad \text{and} \quad \beta'=\mu'/u; \quad \text{(C7)}$$

$$\lambda/3J_{AB}S_AS_B=\tfrac{1}{2}\beta^2uh; \quad \text{(C8)}$$

$$E=2N\lambda[1+\beta^{-2}+\beta'^{-2}]. \quad \text{(C9)}$$

Thus one obtains that value of u for which the chosen value of k is k_0. The remaining spiral parameters ϕ_ν (the cone angles) and γ_ν (the phases) can be found by further evaluating:

$$T=[(1-\beta^2\alpha^2)/(\beta^2\tau^2-1)]^{\frac{1}{2}}; \quad \text{(C10)}$$

$$\phi_1=\phi_2=\tfrac{1}{2}\pi-\cot^{-1}T,$$
$$\phi_3=\phi_4=\tfrac{1}{2}\pi-(\sin\tau')\cot^{-1}(\tau'T/\alpha'), \quad \text{(C11)}$$
$$\phi_5=\phi_6=\tfrac{1}{2}\pi-(\sin\tau)\cot^{-1}(\tau T/\alpha),$$

where the range of the arc cotangent function is defined to be the first and fourth quadrants exclusive of $-\pi/2$; and

$$\gamma_1=\gamma_2=0,$$
$$\gamma_3=\gamma_4=\tfrac{1}{2}\pi[1-\sin(\tau'T/\alpha')], \quad \text{(C12)}$$
$$\gamma_5=\gamma_6=\tfrac{1}{2}\pi[1-\sin(\tau T/\alpha)].$$

APPENDIX IV. THE MATRICES FOR SMALL DEVIATIONS

By means of Eq. (17), it is possible to rewrite Eq. (16) in the form

$$\Delta E=\sum_{\xi,\xi'}\sum_{n\nu,m\mu}F_{n\nu,m\mu}{}^{\xi\xi'}\chi_{n\nu}{}^{\xi}\chi_{m\mu}{}^{\xi'}, \quad \text{(D1)}$$

where

$$F_{n\nu,m\mu}{}^{\xi\xi'}=(\bar{J}_{n\nu,m\mu}-\delta_{n\nu,m\mu}\lambda_{m\mu})\xi_{n\nu}\cdot\xi_{m\mu}'. \quad \text{(D2)}$$

It now becomes convenient to express the components of the small deviations in terms of their Fourier transforms, given by

$$\chi_{n\nu}{}^{\xi}=\sum_{\mathbf{k}}A_\nu{}^{\xi}(\mathbf{k})\exp(i\mathbf{k}\cdot\mathbf{R}_{n\nu}) \quad \text{(D3)}$$

with $\xi=\zeta$, η. Then the change in energy can be written as

$$\Delta E=\sum_{\mathbf{k}}\sum_{\xi,\xi'}\sum_{\nu,\mu}M_{\nu\mu}{}^{\xi\xi'}(\mathbf{k})A_\nu{}^{\xi*}(\mathbf{k})A_\mu{}^{\xi'}(\mathbf{k}), \quad \text{(D4)}$$

where the 12×12 matrix $\mathbf{M}(\mathbf{k})$ is simply the Fourier transform of the matrix $\mathbf{F}$. The explicit evaluation of these matrix elements involves the use of Eq. (D8) given below, and yields:

$$M_{\nu\mu}{}^{\zeta\zeta}(\mathbf{k})=\tfrac{1}{2}\cos\phi_\nu\cos\phi_\mu[\Gamma_{\nu\mu}(\mathbf{k})+\Gamma_{\nu\mu}{}^*(-\mathbf{k})] +\sin\phi_\nu\sin\phi_\mu L_{\nu\mu}(\mathbf{k}),$$
$$M_{\nu\mu}{}^{\zeta\eta}(\mathbf{k})=\tfrac{1}{2}i\cos\phi_\nu[\Gamma_{\nu\mu}(\mathbf{k})-\Gamma_{\nu\mu}{}^*(-\mathbf{k})]=M_{\mu\nu}{}^{\eta\zeta}(\mathbf{k}), \quad \text{(D5)}$$
$$M_{\nu\mu}{}^{\eta\eta}(\mathbf{k})=\tfrac{1}{2}[\Gamma_{\nu\mu}(\mathbf{k})+\Gamma_{\nu\mu}{}^*(-\mathbf{k})],$$

where the $\Gamma_{\nu\mu}$ are obtained from the components of the matrix $\mathbf{L}(\mathbf{k})$, given in Appendix II, according to

$$\Gamma_{\nu\mu}(\pm\mathbf{k})=[L_{\nu\mu}(\pm\mathbf{k}+\mathbf{k}_0)-\delta_{\nu\mu}\lambda_1(\mathbf{k}_0)\beta_\mu{}^{-2}] \times\exp[i(\gamma_\mu-\gamma_\nu)]. \quad \text{(D6)}$$

The eigenvalues $\mu_\alpha(\mathbf{k})$ of the $\mathbf{M}(\mathbf{k})$ matrices are associated with eigenvectors of the form (in the above basis)

$$\Phi_\alpha(\mathbf{k})=C(A_1{}^{\zeta}(\mathbf{k}), A_2{}^{\zeta}(\mathbf{k}), \cdots, A_1{}^{\eta}(\mathbf{k}), A_2{}^{\eta}(\mathbf{k}), \cdots, A_6{}^{\eta}(\mathbf{k})), \quad \text{(D7)}$$

where C is a normalizing constant, and also with $\Phi_\alpha{}^*(\mathbf{k})$, since $\mathbf{M}^*(-\mathbf{k})=\mathbf{M}(\mathbf{k})$. Thus the components of the small deviations along $\boldsymbol{\zeta}_{n\nu}$ and $\boldsymbol{\eta}_{n\nu}$ are directly related to the eigenvectors of $\mathbf{M}(\mathbf{k})$ through Eq. (D3). Furthermore, the coordinate system which "moves" along with the spins $\mathbf{S}_{n\nu}$ is related to the stationary $\hat{x}'$, $\hat{y}'$, $\hat{z}'$ system of Eq. (9) by

$$\boldsymbol{\zeta}_{n\nu}=\cos\phi_\nu[\hat{x}'\cos(\mathbf{k}_0\cdot\mathbf{R}_{n\nu}+\gamma_\nu) +\hat{y}'\sin(\mathbf{k}_0\cdot\mathbf{R}_{n\nu}+\gamma_\nu)]-\hat{z}'\sin\phi_\nu. \quad \text{(D8)}$$
$$\boldsymbol{\eta}_{n\nu}=-\hat{x}'\sin(\mathbf{k}_0\cdot\mathbf{R}_{n\nu}+\gamma_\nu)+\hat{y}'\cos(\mathbf{k}_0\cdot\mathbf{R}_{n\nu}+\gamma_\nu).$$

It follows that, given the eigenvector associated with an eigenvalue, say $\mu_1(\mathbf{k}_1)$, of $\mathbf{M}(\mathbf{k})$, one can straightforwardly calculate the x', y', z' components of the corresponding deviations $\varkappa_{n\nu}$. Thus the Fourier analysis of the resulting deviated spins $\mathbf{S}_{n\nu}'$ will contain contributions from $\pm\mathbf{k}=\mathbf{k}_1$, $\mathbf{k}_0+\mathbf{k}_1$, and $\mathbf{k}_0-\mathbf{k}_1$, in addition to $\pm\mathbf{k}=0$, $\mathbf{k}_0$. If all of these k vectors lie in the "good" set defined in Sec. II, then the results obtained there prove that the deviated configuration must yield a higher energy than the [110] spiral. In other words, instability can only arise when at least one of these k vectors lies in a "bad" set. This information simplifies the examination of local stability, since it restricts the volume of $\mathbf{k}$ space which must be examined.

APPENDIX V. EQUAL-RELATIVE-ANGLE CONFIGURATIONS

Equation (22) defines the class of all configurations possessing the equal-relative-angle property. In order to investigate this entire class, we will need an explicit elucidation of all such configurations, which can be achieved in the form of a classification of permissible Fourier components.

Let us express the $\mathbf{S}_{n\nu}$ in terms of their Fourier transforms $\mathbf{Q}_\nu(\mathbf{k})$, as in Eq. (27) and define $\mathbf{T}_\nu(\mathbf{k})=\mathbf{Q}_\nu(\mathbf{k})\exp(i\mathbf{k}\cdot\boldsymbol{\varrho}_\nu)$. It is also convenient to define $\mathbf{T}_\nu(\mathbf{k})=0$ for all $\mathbf{k}$ not in the first Brillouin zone (BZ), which can be done without any loss of generality because any set of spins can be written in the form of Eq. (27) where the summation goes only over this zone. Then, with $\mathbf{R}_m=\mathbf{R}_n+\mathbf{R}_p$, Eq. (22) becomes for all ν, μ, $\mathbf{R}_n$ and $\mathbf{R}_p$,

$$\sum_{\mathbf{k},\mathbf{k}'}\mathbf{T}_\nu(\mathbf{k})\cdot\mathbf{T}_\mu^*(\mathbf{k}')\exp[i(\mathbf{k}-\mathbf{k}')\cdot\mathbf{R}_n-i\mathbf{k}'\cdot\mathbf{R}_p]=f_{\nu\mu}(\mathbf{R}_p). \quad \text{(E1)}$$

Multiplication of Eq. (E1) by $\exp(i\mathbf{k}''\cdot\mathbf{R}_n)$ and summation over $\mathbf{R}_n$ yields

$$\sum_{\mathbf{k},\mathbf{k}',\mathbf{K}}\delta(\mathbf{k}+\mathbf{k}''-\mathbf{k}',\mathbf{K})\mathbf{T}_\nu(\mathbf{k})\cdot\mathbf{T}_\mu^*(\mathbf{k}')\exp(-i\mathbf{k}'\cdot\mathbf{R}_p)=f_{\nu\mu}(\mathbf{R}_p)\textstyle\sum_{\mathbf{K}}\delta(\mathbf{k}'',\mathbf{K}), \quad \text{(E2)}$$

which must hold for all $\mathbf{k}''$ and for all $\mathbf{R}_p$. [Here $\delta(\mathbf{k},\mathbf{k}')=1$ when $\mathbf{k}=\mathbf{k}'$ and is zero otherwise, and $\mathbf{K}$ is 2π times a reciprocal lattice vector.] The information of interest arises from $\mathbf{k}''\neq\mathbf{K}$, since setting $\mathbf{k}''=\mathbf{K}$ merely gives an expression for $f_{\nu\mu}(\mathbf{R}_p)$. After summing over $\mathbf{k}$ in Eq. (E2), we drop the prime from $\mathbf{k}'$ and obtain

$$\sum_{\mathbf{k},\mathbf{K}}\mathbf{T}_\nu(\mathbf{k}-\mathbf{k}''+\mathbf{K})\cdot\mathbf{T}_\mu^*(\mathbf{k})\exp(-i\mathbf{k}\cdot\mathbf{R}_p)=0 \quad \text{(E3)}$$

for all $\mathbf{k}''\neq\mathbf{K}$. We multiply Eq. (E3) by $\exp(i\mathbf{k}'\cdot\mathbf{R}_p)$ and sum over all $\mathbf{R}_p$. This procedure leads, after a few steps, to

$$\textstyle\sum_{\mathbf{K}}\mathbf{T}_\nu(\mathbf{k}'-\mathbf{k}''+\mathbf{K})\cdot\mathbf{T}_\mu^*(\mathbf{k}')=0 \quad \text{(E4)}$$

for all $\mathbf{k}''\neq\mathbf{K}$. But one can show that, for any value of $\mathbf{k}'-\mathbf{k}''$, there is only one $\mathbf{K}$, say $\mathbf{K}_1$, which will bring $\mathbf{k}'-\mathbf{k}''+\mathbf{K}$ into the BZ. Thus Eq. (E4) is equivalent to requiring that $\mathbf{T}_\nu(\mathbf{k}'-\mathbf{k}''+\mathbf{K}_1)\cdot\mathbf{T}_\mu(\mathbf{k}')=0$ for all $\mathbf{k}''\neq\mathbf{K}$ and all $\mathbf{k}'$. In other words, writing $\mathbf{k}=\mathbf{k}'-\mathbf{k}''+\mathbf{K}_1$,

$$\mathbf{T}_\nu(\mathbf{k})\cdot\mathbf{T}_\mu^*(\mathbf{k}')=0 \quad \text{(E5)}$$

for all $\mathbf{k}$, $\mathbf{k}'$ in BZ with the restriction $\mathbf{k}-\mathbf{k}'\neq\mathbf{K}$. This result contains all our desired information since it is a necessary and sufficient condition for the validity of Eq. (22).

Let us write $\mathbf{T}_\nu(\mathbf{k})=\mathbf{a}_\nu(\mathbf{k})+i\mathbf{b}_\nu(\mathbf{k})$, where $\mathbf{a}$ and $\mathbf{b}$ are real vectors in three-dimensional space. The reality of the spins requires that

$$\begin{aligned}\mathbf{a}_\nu(\mathbf{k})&=\mathbf{a}_\nu(-\mathbf{k}),\\ \mathbf{b}_\nu(\mathbf{k})&=-\mathbf{b}_\nu(-\mathbf{k}),\end{aligned} \quad \text{(E6)}$$

for all $\mathbf{k}\neq\frac{1}{2}\mathbf{K}$, which we shall call "ordinary" k vectors. "Special" k vectors $\boldsymbol{\kappa}=\frac{1}{2}\mathbf{K}$ occur at the origin and at points on the surface of BZ, and in the latter case $-\boldsymbol{\kappa}$ is not in BZ, so that $\mathbf{T}_\nu(-\boldsymbol{\kappa})=0$ for $\boldsymbol{\kappa}$ in BZ. For the "special" k vectors, reality of the spins gives

$$\mathbf{b}_\nu(\boldsymbol{\kappa})=0. \quad \text{(E7)}$$

Furthermore, Eq. (E5) can be rewritten in the form

$$\begin{aligned}\mathbf{a}_\nu(\mathbf{k})\cdot\mathbf{a}_\mu(\mathbf{k}')+\mathbf{b}_\nu(\mathbf{k})\cdot\mathbf{b}_\mu(\mathbf{k}')&=0,\\ \mathbf{a}_\nu(\mathbf{k})\cdot\mathbf{b}_\mu(\mathbf{k}')-\mathbf{b}_\nu(\mathbf{k})\cdot\mathbf{a}_\mu(\mathbf{k}')&=0,\end{aligned} \quad \text{(E8)}$$

for all ν, μ and for all $\mathbf{k}$, $\mathbf{k}'$ in BZ with $\mathbf{k}-\mathbf{k}'\neq\mathbf{K}$.

We can put $\mathbf{k}'=-\mathbf{k}$ and $\nu=\mu$ in the above equation. Using Eq. (E6), we obtain the conditions

$$\begin{aligned}|\mathbf{a}_\nu(\mathbf{k})|^2&=|\mathbf{b}_\nu(\mathbf{k})|^2,\\ \mathbf{a}_\nu(\mathbf{k})\cdot\mathbf{b}_\nu(\mathbf{k})&=0,\end{aligned} \quad \text{(E9)}$$

for all ordinary $\mathbf{k}$ and all ν. We can also choose $\nu=\mu$, but consider all $\mathbf{k}$ and $\mathbf{k}'$ such that $\mathbf{k}\pm\mathbf{k}'\neq\mathbf{K}$. Then both Eq. (E8) and the equation obtained from it by replacing $\mathbf{k}'$ with $-\mathbf{k}'$ hold, implying that

$$\mathbf{a}_\nu(\mathbf{k})\cdot\mathbf{a}(\mathbf{k}')=\mathbf{b}_\nu(\mathbf{k})\cdot\mathbf{b}_\nu(\mathbf{k}')=\mathbf{a}_\nu(\mathbf{k})\cdot\mathbf{b}_\nu(\mathbf{k}')=\mathbf{b}_\nu(\mathbf{k})\cdot\mathbf{a}_\nu(\mathbf{k}')=0 \quad \text{(E10)}$$

for all $\mathbf{k}$, $\mathbf{k}'$ such that $\mathbf{k}\pm\mathbf{k}'\neq\mathbf{K}$. But since $\mathbf{k}$, $\mathbf{k}'$ are in BZ, $\mathbf{k}-\mathbf{k}'=\mathbf{K}$ only if $\mathbf{k}=\mathbf{k}'$, and $\mathbf{k}+\mathbf{k}'=\mathbf{K}$ only if either $\mathbf{k}=-\mathbf{k}'$ or $\mathbf{k}=\mathbf{k}'=\boldsymbol{\kappa}$. Hence the restriction $\mathbf{k}\pm\mathbf{k}'\neq\mathbf{K}$ is satisfied by all ordinary $\mathbf{k}$, $\mathbf{k}'$ such that $\mathbf{k}\neq\pm\mathbf{k}'$. Thus we can combine Eqs. (E9) and (E10) to reach the conclusion that the four vectors $\mathbf{a}_\nu(\mathbf{k})$, $\mathbf{b}_\nu(\mathbf{k})$, $\mathbf{a}_\nu(\mathbf{k}')$, and $\mathbf{b}_\nu(\mathbf{k}')$ must be mutually orthogonal (for a given pair $\mathbf{k}$, $\mathbf{k}'$), which requires at least one of them to be zero. But then Eq. (E9) states that at least two of these vectors, an $\mathbf{a}$ and a $\mathbf{b}$ for the same k vector, must be zero. This argument shows that, within a given sublattice ν, there can be at most one nonzero Fourier component associated with ordinary $\mathbf{k}$'s, a Fourier component being conveniently defined as a pair $[\mathbf{T}_\nu(\mathbf{k}),\ \mathbf{T}_\nu(-\mathbf{k})]$.

Now suppose that $\mathbf{T}_\nu(\mathbf{k})$ and $\mathbf{T}_\mu(\mathbf{k}')$ are nonzero for ordinary $\mathbf{k}$, $\mathbf{k}'$ with $\mathbf{k}\neq\pm\mathbf{k}'$ and $\nu\neq\mu$. An analogous argument again applies, and leads to a contradiction. Hence, we have the following important conclusion: *In any spin configuration satisfying the equal-relative-angle condition of Eq. (22), there can be at most one nonzero ordinary-$\mathbf{k}$ Fourier component, and the k vector must be the same for all ν.* It can also be shown from Eq. (E8) that the set of vectors $\mathbf{a}_\nu(\mathbf{k})$, $\mathbf{b}_\nu(\mathbf{k})$ must be coplanar for all ν, and from Eq. (E9), that they must be of equal length and orthogonal in pairs.

Next we assume that $\mathbf{T}_\nu(\mathbf{k})$ and $\mathbf{T}_\nu(\boldsymbol{\kappa})$ are nonzero, where $\mathbf{k}$ is ordinary and $\boldsymbol{\kappa}$ goes over the set of special k vectors. Then Eqs. (E7) and (E8) yield

$$\begin{aligned}&\mathbf{a}_\nu(\mathbf{k})\cdot\mathbf{a}_\mu(\boldsymbol{\kappa})=\mathbf{b}_\nu(\mathbf{k})\cdot\mathbf{a}_\mu(\boldsymbol{\kappa})=0\\&\mathbf{a}_\nu(\boldsymbol{\kappa})\cdot\mathbf{a}_\mu(\boldsymbol{\kappa}')=0\end{aligned}\qquad\text{(E11)}$$

for all ν, μ, $\boldsymbol{\kappa}$, and $\boldsymbol{\kappa}'$ with $\boldsymbol{\kappa}\neq\boldsymbol{\kappa}'$. The first pair of equations, together with Eq. (E9), shows that all the $\mathbf{a}_\nu(\boldsymbol{\kappa})$ must be collinear. Then the last equation implies that the $\mathbf{a}_\nu(\boldsymbol{\kappa})$ can be nonzero for only one value of $\boldsymbol{\kappa}$, when an ordinary $\mathbf{k}$ is present.

If there is no ordinary-$\mathbf{k}$ component, $\mathbf{T}_\nu(\mathbf{k})=0$ and only the last of Eqs. (E11) remains. This orthogonality condition permits the $\mathbf{a}_\nu(\boldsymbol{\kappa})$ to be nonzero for as many as three different κ vectors. There are no further possibilities.

To summarize, we have shown that every spin configuration which satisfies the translational invariance of the scalar product of a pair of spins for all pairs, as defined by Eq. (22), must belong to one of the following classes:

(*a*) *Simple Spirals.* These are defined as spin configurations for which nonzero Fourier components occur for precisely one ordinary k vector. This k vector is arbitrary and the spins are all parallel to one plane, the orientation of this plane relative either to $\mathbf{k}$ or to the crystal being arbitrary. The other degrees of freedom are the phases of the simple spirals on the various sublattices. The general expression for this class of spin configurations is

$$\mathbf{S}_{n\nu}=\hat{x}'\cos(\mathbf{k}\cdot\mathbf{R}_{n\nu}+\gamma_\nu)+\hat{y}'\sin(\mathbf{k}\cdot\mathbf{R}_{n\nu}+\gamma_\nu),\qquad\text{(E12)}$$

where $\hat{x}'$ and $\hat{y}'$ are orthonormal vectors and the γ_ν are the arbitrary phases.

(*b*) *Ferrimagnetic Spirals.* Here there are nonzero Fourier components for precisely two k-vectors, one of which is the special vector $\mathbf{k}=0$. This class is defined in general by Eq. (9), and is discussed in the text.

(*c*) *Alternating Spirals.* These configurations are similar to (*b*) except that their special vector is a nonzero $\boldsymbol{\kappa}$ at the boundary of the Brillouin zone, instead of the $\boldsymbol{\kappa}=0$. The defining equation is

$$\begin{aligned}\mathbf{S}_{n\nu}=\sin\phi_\nu[&\hat{x}'\cos(\mathbf{k}\cdot\mathbf{R}_{n\nu}+\gamma_\nu)+\hat{y}'\sin(\mathbf{k}\cdot\mathbf{R}_{n\nu}+\gamma_\nu)]\\&+\hat{z}'\cos\phi_\nu\cos(\boldsymbol{\kappa}\cdot\mathbf{R}_n+\gamma_\nu'),\end{aligned}\qquad\text{(E13)}$$

where γ_ν' is either 0 or π, and can depend upon ν. Pictorially, the spins on a given sublattice ν all lie on the surface of a cone with half-angle ϕ_ν, but the cone axis alternates "up and down" as one moves from site to site along the direction of $\boldsymbol{\kappa}$ (since $\boldsymbol{\kappa}\cdot\mathbf{R}_n$ is always a multiple of π).

(*d*) $\boldsymbol{\kappa}$ *Configurations.* In this class there can be one, two, or three special-$\mathbf{k}$ Fourier components, but no ordinary k vectors. The defining equation is

$$\mathbf{S}_{n\nu}=\sum_{p=1}^{3}\mathbf{T}_\nu(\boldsymbol{\kappa}_p)\cos(\boldsymbol{\kappa}_p\cdot\mathbf{R}_n),\qquad\text{(E14)}$$

where the $\mathbf{T}_\nu(\boldsymbol{\kappa}_p)$ are any real vectors which satisfy the conditions $\mathbf{T}_\nu(\boldsymbol{\kappa}_p)\cdot\mathbf{T}_\mu(\boldsymbol{\kappa}_q)=0$ for all ν, μ if $p\neq q$, and $\sum_p|\mathbf{T}_\nu(\boldsymbol{\kappa}_p)|^2=1$. If the configuration contains nonzero Fourier components for three different $\boldsymbol{\kappa}$'s, then it can be expressed as

$$\begin{aligned}\mathbf{S}_{n\nu}=\hat{x}'T_\nu(\boldsymbol{\kappa}_1)\cos(\boldsymbol{\kappa}_1\cdot\mathbf{R}_n)+\hat{y}'T_\nu(\boldsymbol{\kappa}_2)\cos(\boldsymbol{\kappa}_2\cdot\mathbf{R}_n)\\+\hat{z}'T_\nu(\boldsymbol{\kappa}_3)\cos(\boldsymbol{\kappa}_3\cdot\mathbf{R}_n),\end{aligned}\qquad\text{(E15)}$$

with $\sum_p[T_\nu(\boldsymbol{\kappa}_p)]^2=1$, i.e., the $\mathbf{T}_\nu(\boldsymbol{\kappa}_p)$ for a given p must be parallel for all ν. If only two different $\boldsymbol{\kappa}$'s are present, then the $\mathbf{T}_\nu(\boldsymbol{\kappa}_p)$ must be parallel for all ν for one $\boldsymbol{\kappa}$, and must lie in the perpendicular plane for the other $\boldsymbol{\kappa}$. For a single $\boldsymbol{\kappa}$, there is no restriction upon the directions for the various sublattices.

This result completes the elucidation of all possible spin configurations which satisfy the invariance condition of Eq. (22). As far as we know, this is the first time that this class has been obtained explicitly.

Other invariance postulates, more complicated than that of Eq. (22), have been used in the literature.[13,37] For example, Gersch and Koehler elucidated the complete class of Ising (i.e., collinear) configurations on Bravais lattices for which $\mathbf{S}(\mathbf{R})\cdot[\mathbf{S}(\mathbf{R}+\mathbf{R}')+\mathbf{S}(\mathbf{R}-\mathbf{R}')]$ is independent of $\mathbf{R}$. We found that the added complexity makes such an elucidation intractable for spins of more than one dimension even in Bravais lattices.

APPENDIX VI. HIGH-TEMPERATURE APPROXIMATION

According to the molecular field approximation,[38–40] the effect of thermal fluctuations in the directions of the unit spin-vectors $\mathbf{S}_{n\nu}$ can be expressed as an average value given by

$$\langle\mathbf{S}_{n\nu}\rangle=\int\rho_{n\nu}(\mathbf{S})\mathbf{S}\,d\omega,\qquad\text{(F1)}$$

where the integration is over all possible orientations of a unit vector $\mathbf{S}$, each orientation being weighted by the probability density

$$\rho_{n\nu}(\mathbf{S})=Z_{n\nu}^{-1}\exp(\beta\mathbf{S}\cdot\mathbf{H}_{n\nu}).\qquad\text{(F2)}$$

[37] E. F. Bertaut, Compt. rend. **252**, 76 (1961).
[38] J. Villain, J. Phys. Chem. Solids **11**, 303 (1959).
[39] M. Freiser, Phys. Rev. **123**, 2003 (1961).
[40] T. A. Kaplan, Phys. Rev. **124**, 329 (1961).

Here $\beta=1/kT$, the normalization is given by

$$Z_{n\nu}=\int \exp(\beta \mathbf{S}\cdot\mathbf{H}_{n\nu})d\omega, \tag{F3}$$

and the molecular field corresponding to the Heisenberg energy is

$$\mathbf{H}_{n\nu}=-2\sum_{m\mu}\bar{J}_{n\nu,m\mu}\langle\mathbf{S}_{m\mu}\rangle. \tag{F4}$$

The above equations result from approximating the true joint-probability density of a set of spins by a product of independent individual probabilities ($\rho\cong\Pi_{n\nu}\rho_{n\nu}$), and then minimizing the free energy

$$A=\int E\rho d\Omega+kT\int\rho\ln\rho d\Omega \tag{F5}$$

over the $\rho_{n\nu}$.

The transition temperature T_c corresponds to the maximum T for which Eq. (F1) possesses a solution with $\langle\mathbf{S}_{n\nu}\rangle\neq 0$ for some n, ν. For temperatures slightly less than T_c, $\langle\mathbf{S}_{n\nu}\rangle$ will be small and the higher order terms in the expansion of the integrand of Eq. (F1) in powers of $\beta\mathbf{H}_{n\nu}$ can be neglected, giving

$$\langle\mathbf{S}_{n\nu}\rangle=\tfrac{1}{3}\beta\mathbf{H}_{n\nu}=-\tfrac{2}{3}\beta\sum_{m\mu}\bar{J}_{n\nu,m\mu}\langle\mathbf{S}_{m\mu}\rangle. \tag{F6}$$

By substituting the Fourier transforms

$$\langle\mathbf{S}_{n\nu}\rangle=\sum_{\mathbf{k}}\langle\mathbf{Q}_\nu(\mathbf{k})\rangle\exp(i\mathbf{k}\cdot\mathbf{R}_{n\nu}), \tag{F7}$$

multiplying both sides of Eq. (F6) by $\exp(-ik'\cdot R_{n\nu})$, and then summing over n, one obtains

$$\langle\mathbf{Q}_\nu(\mathbf{k})\rangle=-\tfrac{2}{3}\beta\sum_\mu L_{\nu\mu}(\mathbf{k})\langle\mathbf{Q}_\mu(\mathbf{k})\rangle, \tag{F8}$$

where the matrices $L(k)$ are those given in Appendix II. Equation (F8) has the form of an eigenvalue equation, so that nonzero solutions exist if and only if $-\frac{3}{2}kT$ is equal to an eigenvalue of $\mathbf{L}(\mathbf{k})$. Hence T_c is determined by the minimum eigenvalue of $\mathbf{L}(\mathbf{k})$ and the associated eigenvector defines the spin configuration appropriate to T_c.

We have investigated these matrices for the normal cubic spinel with nearest-neighbor A-B and B-B interactions. The minimum eigenvalue of $\mathbf{L}(0)$,

$$\lambda_0=\min_\alpha\lambda_\alpha(0), \tag{F9}$$

is the absolute minimum over all α and $\mathbf{k}$ for all $u\leq u_0(T_c)=2.177$, as shown by calculations over all $\mathbf{k}$ using an IBM 709 computer. The corresponding configuration is of the Néel type, the ratio of the magnitude of $\langle\mathbf{S}_{n\nu}\rangle$ for the B sites ($\nu=3, 4, 5, 6$) to that for the A sites ($\nu=1, 2$) being equal to $|[3u-(9u^2+128)^{\frac{1}{2}}]/16|$. For all $u\geq u_0(T_c)$, the minimum eigenvalue of $\mathbf{L}(k[110]/\sqrt{2})$,

$$\lambda_1(\mathbf{k}_0)=\min_{\alpha,k}\lambda_\alpha(k[110]/2), \tag{F10}$$

is the absolute minimum over all α and $\mathbf{k}$. The associated eigenvector is of the form given in Eq. (B7), and the corresponding configuration is an antiferromagnetic [110] spiral, which of course is degenerate with all its cubic equivalents. The value for $\rho_0=k_0a_0/4\sqrt{2}$ varies from 0.911 at $u_0(T_c)$, through 0.962 at $u=3$, to 1.012 as $u\to\infty$. It is interesting that the above value for ρ_0 at $u_0(T_c)$ is identical with the value for ρ_0 at u_0 when $T=0$.

Since $u_0(T_c)>u''$, it appears that for $u_0\leq u<u''$, there will be at least one transition between $T=T_c$ and $T=0$ if our ferrimagnetic spiral is the ground state. Similarly, for $1.298<u<2.177$, there will be at least two transitions, one between Néel-type and spiral configurations, and another between the spiral and the deviated spiral.